

Contract No:

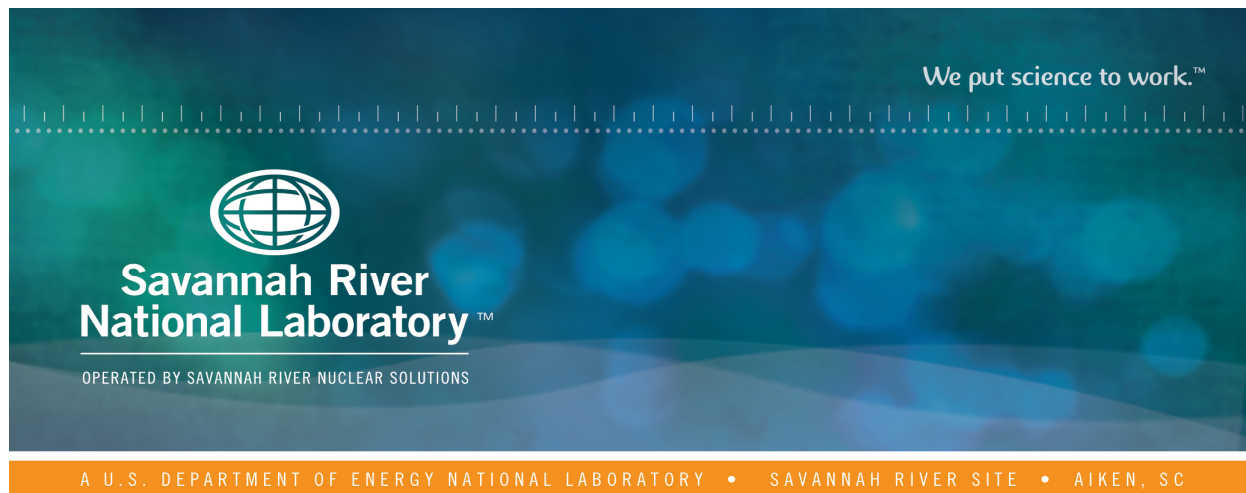
This document was prepared in conjunction with work accomplished under Contract No. DE-AC09-08SR22470 with the U.S. Department of Energy (DOE) Office of Environmental Management (EM).

Disclaimer:

This work was prepared under an agreement with and funded by the U.S. Government. Neither the U. S. Government or its employees, nor any of its contractors, subcontractors or their employees, makes any express or implied:

- 1) warranty or assumes any legal liability for the accuracy, completeness, or for the use or results of such use of any information, product, or process disclosed; or
- 2) representation that such use or results of such use would not infringe privately owned rights; or
- 3) endorsement or recommendation of any specifically identified commercial product, process, or service.

Any views and opinions of authors expressed in this work do not necessarily state or reflect those of the United States Government, or its contractors, or subcontractors.



In-Situ Gamma-Ray Assay of the East Cell Line in the 235-F Plutonium Fuel Form Facility

A.H. Couture – Pajarito Scientific Corporation

D.P. Diprete – Savannah River National Laboratory

July 2015

SRNL-STI-2014-00629 Revision 0



DISCLAIMER

This work was prepared under an agreement with and funded by the U.S. Government. Neither the U.S. Government or its employees, nor any of its contractors, subcontractors or their employees, makes any express or implied:

1. warranty or assumes any legal liability for the accuracy, completeness, or for the use or results of such use of any information, product, or process disclosed; or
2. representation that such use or results of such use would not infringe privately owned rights; or
3. endorsement or recommendation of any specifically identified commercial product, process, or service.

Any views and opinions of authors expressed in this work do not necessarily state or reflect those of the United States Government, or its contractors, or subcontractors.

Printed in the United States of America

**Prepared for
U.S. Department of Energy**

Keywords: 235-F, Non-destructive Assay,
Heat-Source Plutonium, PuFF

Retention: *Permanent*

In-Situ Gamma-Ray Assay of the East Cell Line in the 235-F Plutonium Fuel Form Facility

A.H. Couture
D.P. DiPrete

July 2015

Prepared for the U.S. Department of Energy under
contract number DE-AC09-08SR22470.



EXECUTIVE SUMMARY

On September 17th-19th, 2013, scientists from SRNL took a series of in-situ gamma-ray measurements in the maintenance trench beneath Cells 1-5 on the east line of the PuFF facility using a well-collimated, high-purity germanium detector. The cell interiors were assayed along with the furnaces and storage coolers that protrude beneath the cells. The detector efficiency was estimated using a combination of MCNP simulations and empirical measurements. Data analysis was performed using three gamma-rays emitted by Pu-238 (99.85 keV, 152.7 keV, and 766.4 keV) providing three independent estimates of the mass of Pu-238 holdup in each of the cells. The weighted mean of these three results was used as the best estimate of Pu-238 holdup in the East Cell Line of PuFF. The results of the assay measurements are found in the table on the following page along with the results from the scoping assay performed in 2006 [3]. All uncertainties in this table (as well as the rest of the report) are reported at 1σ . Summing the assay results and treating MDAs as $M_{^{238}\text{Pu}} = 0 \pm \text{MDA}$, the total holdup in the East Cell Line was 240 ± 40 grams. This result is 100 grams lower than the previous estimate, a 0.55σ difference. The uncertainty in the Pu-238 holdup is also reduced substantially relative to the 2006 scoping assay. However, the current assay results are in agreement with the 2006 scoping assay results due to the large uncertainty associated with the 2006 scoping assays. The current assay results support the conclusion that the 2006 results bound the Pu-238 mass in Cells 1-5.

These results should be considered preliminary since additional measurements of the East Cell line are scheduled for 2017 and 2018. Those measurements will provide detailed information about the distribution of Pu-238 in the cells to be used to refine the results of the current assay.

	Current Assay Mass (g)	2006 Scoping Assay Mass (g) [3]
Cell 1 Interior	114 ± 6 (5%)	264.3 ± 166.5 (63%)
Cell 1 North Furnace	17 ± 5 (31%)	Not measured
Cell 1 South Furnace	43 ± 13 (28%)	Not measured
Cell 1 Cooler	10.7 (MDA)	Not measured
Cell 2 Interior	36 ± 3 (9%)	59.7 ± 43.6 (73%)
Cell 2 North Cooler	11.9 ± 1.3 (11%)	Not measured
Cell 2 South Cooler	12.7 (MDA)	Not measured
Cell 3 Interior	2.5 ± 0.4 (16%)	2.17 ± 1.45 (67%)
Cell 3 Cooler	7.3 (MDA)	Not measured
Cell 4 Interior	9.6 ± 0.6 (7%)	9.82 ± 7.27 (74%)
Cell 4 Cooler	22.4 (MDA)	Not measured
Cell 5 Interior	8.7 ± 0.5 (6%)	4.58 ± 3.25 (71%)
Cell 5 Cooler	22.9 (MDA)	Not measured
Cell 5 Furnace	12.4 (MDA)	Not measured
Total East Cell Line	240 ± 40 (17%)	340 ± 170 (50%)

Table ES-0-1: Current Assay Results Compared with the 2006 Scoping Measurements. When tabulating the Total East Cell Line result MDA measurements are included as $M_{238Pu} = 0 \pm MDA$.

TABLE OF CONTENTS

LIST OF TABLES	viii
LIST OF FIGURES	ix
LIST OF ABBREVIATIONS.....	ix
1.0 Introduction.....	1
2.0 Data Collection	2
3.0 MCNP Simulations	4
3.1 Cell Geometry and Materials	4
3.2 Furnace and Cooler Geometry	7
3.3 Cell Source Distributions	9
3.4 Furnace and Cooler Source Distributions.....	11
4.0 Data Analysis	15
4.1 Total Counts	15
4.2 Detector Efficiency.....	17
4.3 Solid Angle and Attenuation Corrections.....	19
4.4 Cross Talk	21
5.0 Assay Results	21
6.0 References.....	28
Appendix A Detector Locations for Cell Interior Assays	30
Appendix B Example MCNP Input Deck.....	32

LIST OF TABLES

Table ES-0-1: Current Assay Results Compared with the 2006 Scoping Measurements	vi
Table 3-1: Dimensions of Cells 1-5 used in the MCNP Simulation	5
Table 3-2: Material Compositions and Densities used in MCNP Simulations	6
Table 3-3: Girder Densities used in MCNP Simulations	6
Table 3-4: Cell Equipment Material Densities used in the MCNP Simulations	7
Table 3-5: Furnace Geometry	8
Table 3-6: Cooler and Furnace Assay Positions	9
Table 3-7: MCNP Flux per Source Photon Results for East Cell Line Interiors	11
Table 3-8: Cell 1 South Furnace MCNP Flux per Source Photon Results	13
Table 3-9: Cell 1 North Furnace MCNP Flux per Source Photon Results	13
Table 3-10: MCNP Flux per Source Photon Results for Coolers and Cell 5 Furnace	14
Table 4-1: Counts in Major Pu-238 Photopeaks for HPGe Measurements	16
Table 4-2: Point Source Efficiencies and Associated Uncertainties	18
Table 5-1: Assay Results for the Three Gamma-Ray Energies.	22
Table 5-2: Sources of Uncertainty for 99.85 keV Analysis	23
Table 5-3: Sources of Uncertainty for 152.7 keV Analysis	24
Table 5-4: Sources of Uncertainty for 766.4 keV Analysis	25
Table 5-5: Current Assay Results compared with 2006 Scoping Measurements [3].....	27
Table 5-6: Conservative Upper Limit for Cell Interior Assays Assuming Pu-238 Distribution on Cell Ceilings.....	27
Table A-6-1: Detector Locations for Cell Interior Assays.....	31

LIST OF FIGURES

Figure 2-1: East Cell Line Geometry and Assay Locations.....	3
Figure 2-2: Map of 153 keV Counts Collected during LaBr Scoping Measurements.....	4
Figure 2-3: Map Showing the Ratio of 99 keV to 153 keV Counts Collected During LaBr Scoping Measurements.....	4
Figure 3-1: Oxygen-Exchange Furnace Vertical Cross Section and Photograph	8
Figure 4-1: Point Source Efficiency for HPGe Detector located 38.1 cm from Ho-166m, Eu-152, Eu-154, and Eu-155 gamma-ray sources.....	17
Figure 4-2: Effect of Collimator of HPGe Detector Efficiency	18

LIST OF ABBREVIATIONS

cm	centimeter
Bq	Becquerel (decays per second)
FWHM	Full-Width at Half-Maximum
HEPA	High-Efficiency Particulate Air (filter)
HPGe	High-Purity Germanium Detector
keV	kilo-electron-Volt
LaBr	Lanthanum Bromide
LANL	Los Alamos National Laboratory
LN	Liquid nitrogen
MCA	Multi-channel Analyzer
MCNP	Monte-Carlo N-Particle Transport Code
MCNP5	Monte-Carlo N-Particle Transport Code, Version 5
mm	millimeter
NDA	Non-destructive Assay
PuFF	Plutonium Fuel Form
PSC	Pajarito Scientific Corporation
SRNL	Savannah River National Laboratory
SRS	Savannah River Site
SS	Stainless Steel
WBS	Work Breakdown Structure

1.0 Introduction

The Plutonium Fuel Form (PuFF) Facility is located in Building 235-F near the geographic center of the Savannah River Site. The facility was used to produce iridium-encapsulated Pu-238 spheres and pellets for use as radioisotope thermal generators, primarily for the space program. The facility is divided between two cell lines, the east cell line used to process the powdered Pu-238 oxide raw material into fuel forms and the west cell line used to encapsulate the fuel forms in iridium. Between 1978 and 1984, the PuFF Facility processed approximately 165 kilograms of Pu-238. In 1984, the facility was placed in “enhanced readiness mode”, which consisted of reducing staff to the minimum required to keep the facility maintained in operating condition while waiting for a new mission. During this time, the inert argon atmosphere in the east cell line was not maintained. The purpose of the inert argon atmosphere was to prevent corrosion from the high-alpha activity of Pu-238. Corrosion soon made the East Cell Line inoperable, particularly the aluminum remote manipulators. The facility has not been decontaminated since the intent was to continue operations and after the failure of the manipulators much of the facility is inaccessible [1].

Scoping in-situ gamma-ray assays were performed in the PuFF Facility in 2006 [3]. The current estimate of Pu-238 holdup in the facility is based upon these measurements. Using this holdup estimate as a source term, SRS has performed a risk analysis that indicated a seismic event that induces a full-facility fire in 235-F could lead to a 28,800 rem dose to a co-located worker [6]. Based on this risk assessment, SRS is taking steps to decontaminate the facility. One of the first steps taken has been to improve upon the quality of the in-situ gamma-ray assay data. Carts and collimators were specially designed to survey the equipment in the PuFF Facility. While the previous scoping work consisted of 32 measurements [3], the current series of assay measurements included nearly 400 measurements, with most of this increase occurring on the East Cell Line. Data analysis for the current set of measurements was conducted with greater rigor as well. MCNP5 [2] was used to evaluate a variety of possible physical distributions for the Pu-238 source term and estimate cross-talk between neighboring cells. This report describes the East Cell Line hold-up measurements and subsequent data analysis.

This report is in direct support of the following WBS elements as defined by the Deactivation Project Plan for the 235-F PuFF Facility [10]:

- 01.29.24.01.09.05, Develop Method/Design for Enhanced Characterization, Cells 3-9
- 01.29.24.01.14.02, Develop Method/Design for Enhanced Characterization, Cells 1-2
- 01.29.24.01.15.04, Perform Enhanced Characterization of Cells 3-5
- 01.29.24.01.16.05, Perform Enhanced Characterization of Cells 1-2

Per the Deactivation Project Plan, the above WBS elements provide for "enhanced characterization" of Cells 1-5 prior to intrusive deactivation activities such as material removal and decontamination. This report documents one component (exterior measurements coupled with MCNP modeling) of the planned initial, enhanced characterization of Cell 1-5. Other components (e.g., in-cell measurements or measurements through partially disassembled shield windows) of the initial, enhanced characterization are planned for FY17 and FY18 with results to be documented in separate, future reports.

2.0 Data Collection

On September 17th-19th, 2013, scientists from SRNL took a series of in-situ gamma-ray measurements in the maintenance trench beneath Cells 1-5 on the East Cell Line of the PuFF facility. The detector used was a 20%-efficient, p-type HPGe detector with a 1.27 mm aluminum endcap. The detector's efficiency calibration was verified on the day of the measurements using a Cs-137 check source. A Canberra Lynx MCA was used to provide high-voltage and preamplifier power to the detector as well as process the detector signals. A Panasonic TOUGHBOOK tablet computer was used to run Canberra's Genie 2000 software [13], which controlled the MCA and saved the spectral data. A specialized cart was fabricated to hold the detector in a vertical orientation, aimed at the floor of the cells above. A second cart was used to hold the detector in a horizontal orientation to assay the furnaces and coolers that protruded beneath the cell floors. The detector, LN dewar, signal cables, Lynx MCA, and tablet computer were all wrapped in plastic to prevent Pu-238 contamination. A large tungsten-shot collimator was used for all data acquisitions. The tungsten shot collimator was a stainless steel canister that shielded the sides of the detector crystal with 4.2 cm of tungsten shot and the face with 10.16 cm. The hole in the collimator was 4.12 cm in diameter, which narrowed the detector's view of the floor to a roughly 75 cm diameter circular region. A tungsten shot plug was used to occlude the collimator hole for background measurements. All spectra taken in the vertical orientation had negligible Pu-238 backgrounds. All spectral acquisitions

were taken with two minutes live time, however the northern furnace in Cell 1 was assayed four times consecutively in the same location. Twenty-nine spectra were taken of the Cell 1 floor, ten of Cell 2, ten of Cell 3, thirteen of Cell 4, and seven of Cell 5. A diagram showing the approximate location of each floor measurement in relation to the East Cell Line geometry is shown in Figure 2-1. A table containing the coordinates of these locations may be found in Appendix A. Measurements were taken of all oxygen exchange furnaces and coolers except the Cell 5 cooler, which was inaccessible with the horizontal detector cart. The southern end of Cell 5 was inaccessible to the vertical detector cart because the access stairs to the maintenance trench are in the way.

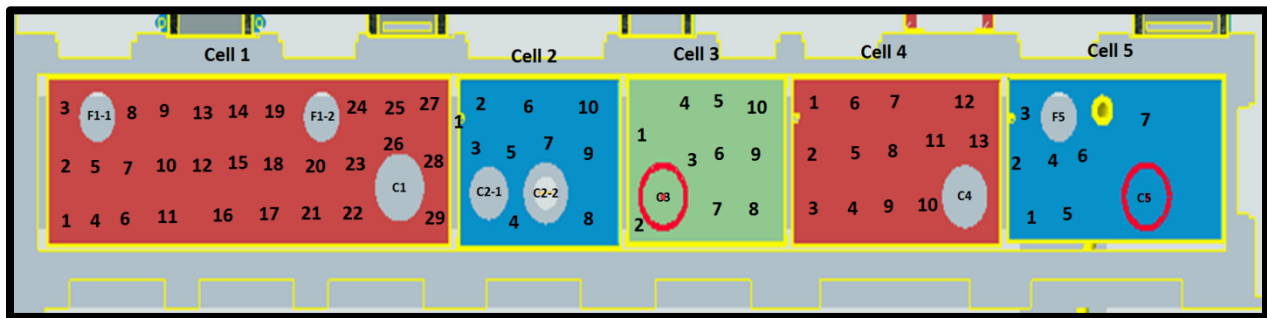


Figure 2-1: East Cell Line Geometry and Assay Locations. The assay locations in each cell are indicated by numbers. Oxygen-exchange furnaces and coolers are labeled with F or C, respectively, followed by the cell number. If there are multiple furnaces or coolers in the cell, the label is appended with -1 or -2. Cell 1 is on the northern end of the cell line.

Between August 12th and 15th, 2013 a series of scoping measurements were performed using a tightly-collimated LaBr detector. Sixty-eight measurements were taken with the detector pointed up at the cell floors. These measurements each had a view of a roughly 40 cm diameter region of the cell floors. Thirty-eight measurements were taken examining the furnaces and coolers that protrude beneath the cell floors. During each of these measurements data were acquired for thirty seconds live time. For the most part, these measurements were not used directly in data analysis, but were instead used as supporting evidence for likely distributions of Pu-238 in the East Cell Line. Figures 2-2 and 2-3 show maps of the 153 keV count rate and the ratio of 99 keV counts to 153 keV counts acquired during the LaBr measurements, respectively. These measurements indicate that the Pu-238 is distributed fairly evenly throughout the cells. The ratio map indicates that the attenuation is relatively uniform as well; there are not locations with significantly more shielding than others.

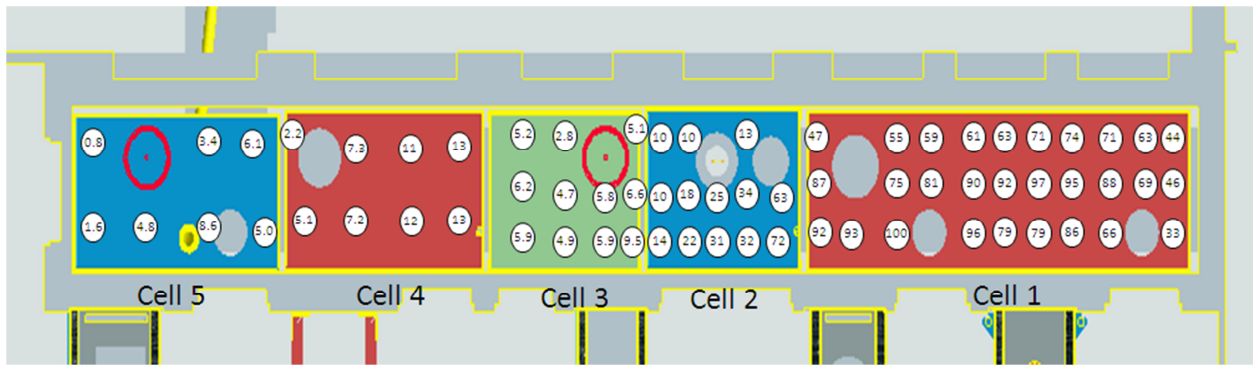


Figure 2-2: Map of 153 keV Counts Collected during LaBr Scoping Measurements. The circles approximate the collimator view. Counts are normalized such that the location with the highest count rate is labeled “100”. To obtain the total 153 keV counts for a measurement, multiply the label by a factor of 576.8.

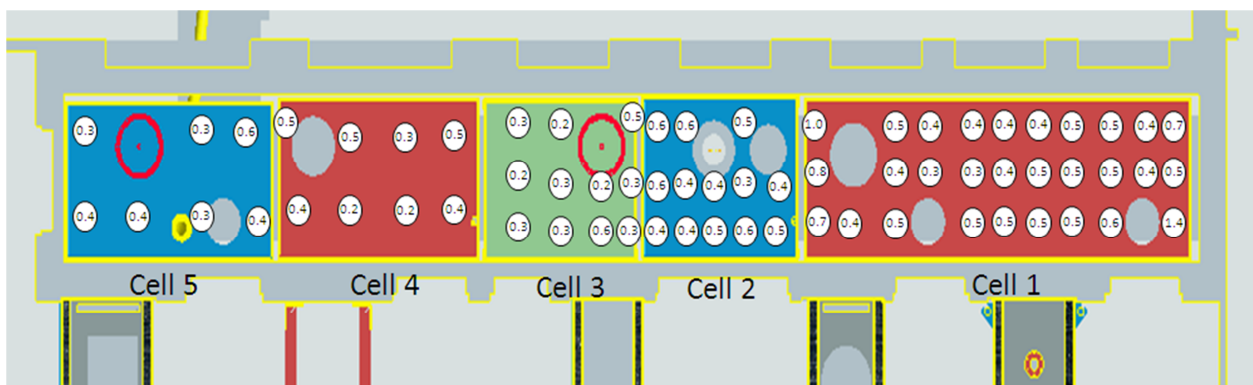


Figure 2-3: Map Showing the Ratio of 99 keV to 153 keV Counts Collected During LaBr Scoping Measurements.

3.0 MCNP Simulations

To estimate the gamma-ray flux at the detector locations per gamma-ray emitted by Pu-238, a simulation of the east cell line of PuFF was created using the MCNP5 [2] software. This program was used to determine the geometric solid angle of the detector relative to the source geometry as well as correct for attenuation of the gamma-ray flux through intervening material in the cells.

3.1 Cell Geometry and Materials

Cells 1-5 were modeled as five box-shaped enclosures composed of 316 stainless steel with dimensions based on SRS engineering drawings [4,5]. The walls and ceilings were modeled as 3.2 mm thick and the

floor was 4.76 mm thick. The interior dimensions of the cells are given in Table 3-1. There are 11.11 cm gaps between adjacent cell walls. The material compositions and densities used in the simulation were taken from Reference 11. These compositions are summarized in Table 3-1. The cell floors are supported from below by a mesh pattern of 3-inch, C-channel, carbon steel girders with a linear density of 4.1 pounds per foot. Rather than include the complicated details of this mesh pattern in the simulation, the attenuation arising from the girders was included by approximating the girder geometry as a uniform, 7.62 cm layer of carbon steel with the same mass as the girders. The overall length of girders beneath each cell was estimated from engineering drawings [4,5] and used to derive the density of the girder layer for each cell. Table 3-3 contains the estimated girder lengths and effective densities used in the MCNP simulation. The HEPA filters were modeled as borosilicate fiberglass encased within a 3 mm thick steel shell. Materials on the cell floor (storage container, ball mills, etc) were simulated as a uniform layer of stainless steel from the cell floor to a height of 30 cm. The material inventory in the cells was estimated from photographic evidence, engineering drawings [4,5], and discussions with SRS employees [7]. A high-, middle-, and low-density estimate was made for this material layer to account for the cell inventories. These estimates are found in Table 3-4. The detector collimator was modeled as a uniform mass of 70% tungsten, 20% nickel, and 10% iron (by mass) with a bulk density of 9.6 g/cm³. The exterior steel shell was not modeled, however the steel in the collimator hole was modeled explicitly. The collimator/detector locations used in MCNP calculations may be found in Appendix A.

Cell	Length (cm)	Width (cm)	Height (cm)
1	512.45	152.4	208.28
2	201.93	152.4	208.28
3	201.93	152.4	208.28
4	263.84	152.4	208.28
5	274.32	152.4	208.28

Table 3-1: Dimensions of Cells 1-5 used in the MCNP Simulation. Length is along the north-south axis, width along the east-west axis.

Material	Density (g/cm ³)	Element	Mass or Atom* Fraction
Stainless Steel 316	7.92**	Silicon	0.010
		Chromium	0.170
		Manganese	0.020
		Iron	0.655
		Nickel	0.120
		Molybdenum	0.025
Carbon Steel	7.82**	Carbon	0.005
		Iron	0.995
Water	1.0	Hydrogen	0.666667*
		Oxygen	0.333333*
Borosilicate Fiberglass	0.02	Boron	0.040063
		Oxygen	0.539561
		Sodium	0.028191
		Aluminum	0.011644
		Silicon	0.377220
		Potassium	0.003321
Lead	11.34	Lead	1.0
Aluminum Oxide	3.85**	Oxygen	0.6*
		Aluminum	0.4*
Tungsten	19.3**	Tungsten	1.0
Air	0.001205	Carbon	0.00124
		Nitrogen	0.755268
		Oxygen	0.231781
		Argon	0.012827
Tungsten Shot	9.6	Iron	0.1
		Nickel	0.2
		Tungsten	0.7

Table 3-2: Material Compositions and Densities used in MCNP Simulations. Elemental compositions are given by mass fraction except for those indicated by an asterisk (*) that were given by atom fraction. Densities marked with a double asterisk (**) were varied in the geometry to simulate a group of discrete items as a uniform layer of material with a lower density. Elemental compositions were taken from Reference 11.

Cell	Estimated Girder Length (ft)	MCNP Girder Density (g/cm ³)
1	96	0.321
2	50	0.393
3	40	0.315
4	47	0.286
5	24	0.150

Table 3-3: Girder Densities used in MCNP Simulations. Floor support girders were simulated as a uniform layer of carbon steel 7.62 cm thick directly beneath the cell floors.

Cell	Low Density Estimate (g/cm ³)	Middle Density Estimate (g/cm ³)	High Density Estimate (g/cm ³)
1	0.045	0.083	0.122
2	0.025	0.044	0.064
3	0.007	0.020	0.032
4	0.009	0.026	0.043
5	0.049	0.083	0.118

Table 3-4: Material Densities used in MCNP Simulations to Account for Cell Equipment Inventories. Material inventory within each of the cells was simulated as a uniform layer of stainless steel directly above the cell floor 30 cm thick.

3.2 Furnace and Cooler Geometry

The East Cell Line of the PuFF facility contains three oxygen exchange furnaces designed to reduce the neutron dose arising from (α ,n) reactions in the plutonium oxide by replacing natural oxygen with enriched O-16. The three furnaces are essentially identical. A cross sectional drawing of the furnaces, as well as a picture of one is included in Figure 3-1. The furnace contains multiple layers of various materials. These layers are from outer to inner: a skin layer, an outer shell, an inner shell, alumina bubble insulation, a heater element, a heater tube, and a work tube. The alumina bubble insulation consists of small spherical shells of aluminum oxide. The bulk density of this layer is unknown. However, based on current manufacturer information, high (1.04 g/cm³), middle (0.76 g/cm³), and low (0.48 g/cm³) density simulations were run for this layer. Table 3-5 gives the material of composition and geometry of these layers. Inside the work tube is the hearth, a removable interior section that contains aluminum oxide insulation and supports the sample holder. There are no drawings or pictures of the sample holder. It is an aluminum oxide rack that held either trays of powdered or pelletized Pu-238. The sample holder was modeled as a cylindrical region of aluminum oxide almost filling the work tube beneath the hearth. The bulk density of the sample holder was varied between 0 and 0.68 g/cm³ in the models. The Cell 1 furnaces were assayed from outside the maintenance trench and the top portion of the furnace was shielded by the doorframe (see the photograph in Figure 3-1) The door frame, which consisted of a steel liner filled with limonite concrete and a lead plate, was included in the model. The doorframe was completely opaque to Pu-238 photons.

Layer	Material	OD (cm)	Thickness (cm)	Lower z-coordinate (cm)	Height (cm)
Skin	SS	17.28	0.12	-79.02	79.02
Outer Shell	SS	16.85	0.56	-78.38	78.38
Inner Shell	SS	15.88	0.31	-78.38	78.38
Alumina Bubble	Al ₂ O ₃	15.57	7.95	-77.27	77.27
Heater Element	Tungsten	7.77	0.15	-64.57	36.14
Heater Tube	Al ₂ O ₃	7.62	0.63	-67.11	67.11
Work Tube	Al ₂ O ₃	6.67	0.64	-64.57	64.57

Table 3-5: Furnace Geometry. The lower z-coordinate is referenced relative to the top of the furnace, which is at the same level as the cell floor. Please note that the alumina bubble layer has two slightly different thicknesses. Its inner boundary is defined partially by the heater element and partially by the heater tube.

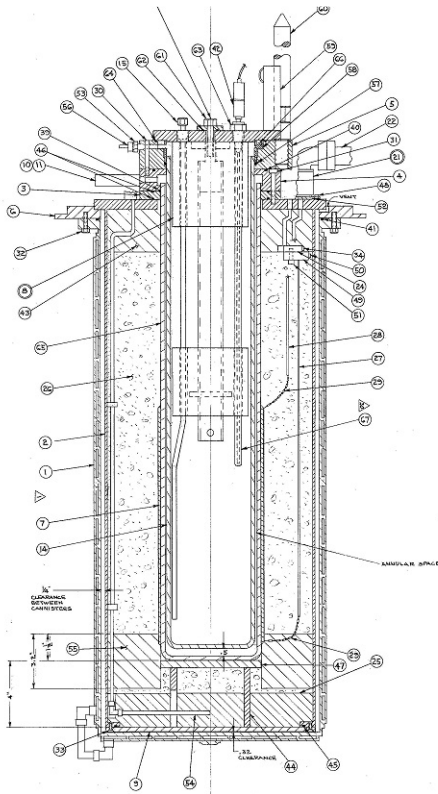


Figure 3-1: Oxygen-Exchange Furnace Vertical Cross Section and Photograph

Each cooler in Cells 1-5 is different. The coolers in Cells 1 and 2 were modeled explicitly as shown in their mechanical drawings [4,5]. Since the count rates observed were at background levels during measurements of the Cell 3, 4 and 5 coolers, the cooler geometry was simplified for the purposes of

determining an order-of-magnitude MDA. The coolers in Cells 3, 4, and 5 were modeled as stainless steel cylinders with an external radius of 27.94 cm and a wall thickness of 1.51 cm extending 59.96 cm beneath the cell floors. The coolers have the same exterior dimensions as the model, however they contain six cylindrical chambers that would store the Pu-238. Rather than modeling these chambers explicitly, the outer wall thickness in the model is the sum of the wall thicknesses of the interior chambers and the outer shell. The interior of the coolers were modeled completely filled with water.

The coolers and furnaces were assayed with the detector and collimator in a horizontal position. The collimator composition and geometry was treated identically with the cell floor measurements. The standoff (from the surface) and vertical distance beneath the cell floor for each assay location are in Table 3-6.

Assay	Standoff (cm)	Vertical Position (cm)
Cell 1 North Furnace	200.16	45.72
Cell 1 South Furnace	145.55	45.72
Cell 1 Cooler	49.53	55.09
Cell 2 North Cooler	35.56	41.12
Cell 2 South Cooler	71.12	42.07
Cell 3 Cooler	71.12	41.75
Cell 4 Cooler	74.12	41.75
Cell 5 Furnace	142.24	41.75

Table 3-6: Cooler and Furnace Assay Positions. Standoffs are given from the detector face to the outer surface of the assayed object. The vertical position is the distance beneath the plane of the cell floor. Please note that the Cell 5 Cooler was not assayed using the HPGe detector. It was only measured with the LaBr detector.

3.3 Cell Source Distributions

The photon sources modeled in the MCNP simulation all emitted gamma-rays at three discrete energies, 99.85 keV, 152.7 keV, and 766.4 keV. Photons were directed towards the collimators in the simulation with a maximum angle of 25.84° with respect to the negative vertical axis. This is five percent of the solid angle for an isotropic source. Photons emitted above this angle were unable to penetrate the collimator. This was done to decrease the computer time required by not simulating photons that were unable to interact with the detectors. All the results from these simulations must be multiplied by three

since the source was split between three gamma rays and divided by twenty to account for the reduced solid angle. A variety of source distributions were modeled to estimate the uncertainty in the overall detector efficiency arising from gamma attenuation and solid angle effects. The source distributions were applied to each cell one at a time. The following source distributions were modeled:

Floor: Photon source uniformly distributed on the floor of the cells,

Uniform: Photon source uniformly distributed throughout the volume of each cell above the middle-density material layer described in Table 3-4 representing an airborne distribution,

Material Layer (ML): Photon source uniformly distributed throughout the middle-density material layer described in Table 3-4,

High Material Layer (HML): Photon source uniformly distributed throughout the high-density material layer described in Table 3-4,

Low Material Layer (LML): Photon source uniformly distributed throughout the low-density material layer described in Table 3-4,

Ceiling Material Layer (CML): Photon source uniformly distributed on the ceiling of the cells with the middle-density material layer described in Table 3-4 acting as an attenuator,

Wall Material Layer (WML): Photon source uniformly distributed on the walls of the cells with the middle-density material layer described in Table 3-4 acting as an attenuator,

and **HEPA:** Photon source uniformly distributed within the HEPA filter in each cell with the middle-density material layer described in Table 3-4 acting as an attenuator.

Based upon LaBr scoping measurements as well as the HPGe assay, there is no evidence of Pu-238 being concentrated on either the cell walls or the HEPA filters. The detectors were well collimated such that only certain measurements had a view of these structures. The measurements that were sensitive to material on the walls and HEPAs showed no statistical increase in activity over neighboring measurements. If future in-cell measurements are able to discern the ratio of material on the walls and HEPAs to material distributed on the cell floors, the results of these MCNP calculations may be used to modify the current assay results accordingly. The assay results are based upon the Floor, Material Layer, High Material Layer, and Low Material Layer source distributions. The Uniform source distribution was not included as only a minute fraction of the Pu-238 should be airborne. Though it is unlikely that any significant amount of Pu-238 is distributed on the ceiling of the cells, calculations were made assuming that all of the material was located on the ceiling as a conservative upper limit on the assay mass. Table 3-7 contains the MCNP flux at the face of the detectors per source photon calculations for the source distributions used in calculations of the assay masses in the East Cell Line. The flux calculations for the

cells treat the multiple measurements beneath each cell as a detector array rather than a sequence of independent measurements.

Distribution	Cell 1	Cell 2	Cell 3	Cell 4	Cell 5
99 keV Flux (cm-2)					
Floor	4.05E-07	2.46E-07	3.33E-07	3.71E-07	2.86E-07
ML	2.65E-07	1.92E-07	2.97E-07	3.18E-07	1.86E-07
HML	2.23E-07	1.74E-07	2.79E-07	2.92E-07	1.58E-07
LML	3.18E-07	2.12E-07	3.18E-07	3.49E-07	2.18E-07
CML	1.26E-07	9.97E-08	1.85E-07	2.02E-07	8.29E-08
153 keV Flux (cm-2)					
Floor	1.22E-06	8.32E-07	1.02E-06	1.09E-06	6.96E-07
ML	9.67E-07	7.28E-07	9.52E-07	1.00E-06	5.51E-07
HML	8.77E-07	6.90E-07	9.22E-07	9.57E-07	5.05E-07
LML	1.07E-06	7.66E-07	9.86E-07	1.05E-06	6.02E-07
CML	5.92E-07	4.29E-07	6.36E-07	6.88E-07	3.19E-07
766 keV Flux (cm-2)					
Floor	3.09E-06	2.25E-06	2.58E-06	2.70E-06	1.53E-06
ML	2.80E-06	2.09E-06	2.48E-06	2.58E-06	1.38E-06
HML	2.70E-06	2.05E-06	2.45E-06	2.54E-06	1.33E-06
LML	2.91E-06	2.13E-06	2.51E-06	2.63E-06	1.42E-06
CML	1.92E-06	1.28E-06	1.62E-06	1.78E-06	8.88E-07

Table 3-7: MCNP Flux per Source Photon Results for East Cell Line Interiors. This table gives the total flux at the detector face for all measurements beneath a particular cell.

3.4 Furnace and Cooler Source Distributions

As with the cell simulations, the photon sources modeled in the MCNP simulation all emitted gamma-rays at three discrete energies, 99.85 keV, 152.7 keV, and 766.4 keV. Photons were directed from the two furnaces in Cell 1 towards the collimator in the simulation with a maximum angle of 25.84° with respect to the horizontal x-axis. This is five percent of the solid angle for an isotropic source. Photons emitted above this angle were unable to penetrate the collimator. This was done to decrease the computer time required by not simulating photons that were unable to interact with the detectors. All the results

from these simulations must be multiplied by three since the source was split between three gamma rays and divided by twenty to account for the reduced solid angle. In the Cell 1 furnaces, a variety of source distributions were modeled to estimate the uncertainty in the overall detector efficiency arising from gamma attenuation and solid angle effects. The following source distributions were modeled and if not explicitly stated the mid-range density was used for any item where the density varied:

Work Tube Bottom (WTB): Photon source distributed uniformly on the bottom surface of the work tube

Work Tube Walls (WTW): Photon source distributed uniformly on the walls of the work tube beneath the hearth

Hearth: Photon source uniformly distributed on the inner wall of the hearth

Sample Holder (SH): Photon source uniformly distributed throughout the volume of the sample holder region

Low Sample Holder (LSH): Photon source uniformly distributed throughout the volume of the sample holder region using the low-range density (0 g/cm^3) for the sample holder

High Sample Holder (HSH): Photon source uniformly distributed throughout the volume of the sample holder region using the high-range density (0.68 g/cm^3) for the sample holder

Low Alumina Bubbles (LAB): Photon source uniformly distributed throughout the volume of the sample holder region the low-range density (0.48 g/cm^3) for the alumina bubble insulation

High Alumina Bubbles (HAB): Photon source uniformly distributed throughout the volume of the sample holder region the high-range density (1.04 g/cm^3) for the alumina bubble insulation

The results of the MCNP flux per source photon calculations for the various source distributions in the South and North Furnaces in Cell 1 are found in Tables 3-8 and 3-9, respectively.

Distribution	99 keV Flux (cm⁻²)	153 keV Flux (cm⁻²)	766 keV Flux (cm⁻²)
WTB	1.14E-10	8.68E-09	3.00E-07
WTW	3.54E-11	7.85E-09	3.15E-07
Hearth	2.16E-09	1.29E-08	1.28E-07
SH	5.94E-11	1.11E-08	3.60E-07
LSH	7.56E-11	1.36E-08	4.02E-07
HSH	4.60E-11	9.00E-09	3.20E-07
LAB	8.37E-11	1.50E-08	4.22E-07
HAB	4.12E-11	8.27E-09	3.07E-07

Table 3-8: Cell 1 South Furnace MCNP Flux per Source Photon Results

Distribution	99 keV Flux (cm⁻²)	153 keV Flux (cm⁻²)	766 keV Flux (cm⁻²)
WTB	1.54E-10	1.41E-08	5.02E-07
WTW	6.18E-11	1.42E-08	5.70E-07
Hearth	3.55E-09	2.15E-08	2.21E-07
SH	1.05E-10	2.03E-08	6.59E-07
LSH	1.33E-10	2.49E-08	7.35E-07
HSH	8.16E-11	1.64E-08	5.86E-07
LAB	1.49E-10	2.73E-08	7.73E-07
HAB	7.16E-11	1.51E-08	5.61E-07

Table 3-9: Cell 1 North Furnace MCNP Flux per Source Photon Results

For the coolers and the Cell 5 furnace, much simpler source distributions were assumed. Measured count rates from these objects were beneath or just at the edge of the MDA level. The MCNP simulation for the coolers in Cells 1 and 2 use point sources located 3 cm above the bottom of each of the wells used to contain the Pu-238. The coolers in Cells 3, 4, and 5 use point sources located at the geometric center of the cylinder used to approximate the cooler geometry. The Cell 5 furnace uses a point source located 3 cm above the floor of its work tube. The results of the MCNP flux per source photon calculations for the coolers and the Cell 5 furnace are found in Table 3-10.

Object	99.85 keV Flux (cm ⁻²)	152.7 keV Flux (cm ⁻²)	766.4 keV Flux (cm ⁻²)
Cell 1 Cooler	4.2E-09 ± 5%	4.95E-08 ± 1.5%	5.20E-07 ± 0.5%
Cell 2 North Cooler	2.5E-08 ± 2%	2.35E-07 ± 0.7%	2.14E-06 ± 0.2%
Cell 2 South Cooler	0	0	3.33E-07 ± 0.6%
Cell 3 Cooler	2.2E-09 ± 13%	2.03E-8 ± 4%	4.17E-07 ± 0.9%
Cell 4 Cooler	8.2E-10 ± 20%	1.16E-08 ± 5%	2.97E-07 ± 1.1%
Cell 5 Furnace	5.7E-11 ± 50%	1.02E-09 ± 3%	3.63E-09 ± 0.6%

Table 3-10: MCNP Flux per Source Photon Results for Coolers and Cell 5 Furnace. Uncertainties are from MCNP statistics only. Please note that the Cell 2 South Cooler is shielded with 0.64 cm of lead, while the other coolers are not. The MCNP simulation was not run long enough to obtain statistically significant results for the 99.85 keV and 152.7 keV gamma-rays.

4.0 Data Analysis

To calculate the mass of Pu-238 in the Cells 1-5 assays the following formula was used:

$$M_{^{238}\text{Pu}} = \frac{N_{net}}{S_{^{238}\text{Pu}} \cdot BR_{\gamma} \cdot \varepsilon \cdot t} \quad \text{Equation 4-1}$$

where,

N_{net} = the net counts in the photopeak used in the analysis for the system of detectors beneath the cell in question (or the minimum detectable count if applicable),

$S_{^{238}\text{Pu}}$ = the specific activity of Pu-238 (6.336×10^{11} Bq/gram \pm 0.1%),

BR_{γ} = the absolute branching ratio of the gamma-ray used for the analysis,

t = the assay live time,

ε = the detector efficiency at the energy of the gamma-ray used for the analysis.

4.1 Total Counts

The three major gamma-rays emitted by Pu-238 were used for the analysis: 99.85 keV, 152.7 keV, and 766.4 keV. PeakEasy 4.51 [8] software developed by LANL was used to fit and integrate the three photopeaks in each measured spectrum. Table 4-1 contains the photopeak integrals and uncertainties for each sequence of assay measurements. Background spectra were acquired using a collimator plug. There were no counts in the background spectra for any of the measurements made in the vertical orientation (looking at the cell floors) or for the two furnaces in Cell 1. MDAs were calculated using the standard Currie formula [9]:

$$MDA = 2.71 + 4.65\sqrt{\sigma_{GROSS}^2 + \sigma_{BKG}^2}.$$

Assay Location	99.85 keV Counts	152.7 keV Counts	766.4 keV Counts
Cell 1 Interior	$3.569 \times 10^6 \pm 0.06\%$	$1.249 \times 10^6 \pm 0.1\%$	$2.01 \times 10^3 \pm 1.3\%$
Cell 1 North Furnace*	$3.25 \times 10^4 \pm 0.7\%$	$1.80 \times 10^4 \pm 0.9\%$	$640 \pm 6\%$
Cell 1 South Furnace	$2.69 \times 10^4 \pm 0.7\%$	$1.36 \times 10^4 \pm 1.0\%$	$770 \pm 4\%$
Cell 1 Cooler GROSS	$5.312 \times 10^5 \pm 0.2\%$	$2.351 \times 10^5 \pm 0.2\%$	$5.76 \times 10^3 \pm 2\%$
Cell 1 Cooler BKG	$5.293 \times 10^5 \pm 0.2\%$	$2.323 \times 10^5 \pm 0.2\%$	$5.44 \times 10^3 \pm 2\%$
Cell 1 Cooler	5.5×10^3 (MDA)	3.6×10^3 (MDA)	650 (MDA)
Cell 2 Interior	$5.836 \times 10^5 \pm 0.16\%$	$2.314 \times 10^5 \pm 0.3\%$	$4.8 \times 10^3 \pm 3\%$
Cell 2 North Cooler GROSS	$1.187 \times 10^6 \pm 0.1\%$	$5.033 \times 10^5 \pm 0.2\%$	$1.15 \times 10^4 \pm 1\%$
Cell 2 North Cooler BKG	$1.156 \times 10^6 \pm 0.1\%$	$4.874 \times 10^5 \pm 0.2\%$	$1.10 \times 10^4 \pm 1\%$
Cell 2 North Cooler	$3.2 \times 10^4 \pm 5\%$	$1.6 \times 10^4 \pm 7\%$	800 (MDA)
Cell 2 South Cooler GROSS	$5.88 \times 10^4 \pm 0.5\%$	$2.86 \times 10^4 \pm 0.6\%$	$640 \pm 5\%$
Cell 2 South Cooler BKG	$5.83 \times 10^4 \pm 0.5\%$	$2.83 \times 10^4 \pm 0.6\%$	$670 \pm 5\%$
Cell 2 South Cooler	1.8×10^3 (MDA)	1.3×10^3 (MDA)	210 (MDA)
Cell 3 Interior	$4.65 \times 10^4 \pm 0.7\%$	$1.72 \times 10^4 \pm 1.2\%$	$380 \pm 14\%$
Cell 3 Cooler GROSS	$3.45 \times 10^4 \pm 0.6\%$	$1.91 \times 10^4 \pm 0.8\%$	$610 \pm 5\%$
Cell 3 Cooler BKG	$3.46 \times 10^4 \pm 0.6\%$	$1.86 \times 10^4 \pm 0.8\%$	$610 \pm 5\%$
Cell 3 Cooler	1.4×10^3 (MDA)	1.0×10^3 (MDA)	190 (MDA)
Cell 4 Interior	$1.883 \times 10^5 \pm 0.3\%$	$7.48 \times 10^4 \pm 0.4\%$	$1.44 \times 10^3 \pm 5\%$
Cell 4 Cooler GROSS	$1.456 \times 10^5 \pm 0.3\%$	$7.11 \times 10^4 \pm 0.4\%$	$1.94 \times 10^3 \pm 3\%$
Cell 4 Cooler BKG	$1.463 \times 10^5 \pm 0.3\%$	$7.16 \times 10^4 \pm 0.4\%$	$1.93 \times 10^3 \pm 3\%$
Cell 4 Cooler	2.9×10^3 (MDA)	1.9×10^3 (MDA)	320 (MDA)
Cell 5 Interior	$7.99 \times 10^4 \pm 0.4\%$	$3.47 \times 10^4 \pm 0.6\%$	$640 \pm 7\%$
Cell 5 Furnace GROSS	$4.13 \times 10^4 \pm 0.6\%$	$2.37 \times 10^4 \pm 0.7\%$	$850 \pm 4\%$
Cell 5 Furnace BKG	$4.12 \times 10^4 \pm 0.6\%$	$2.33 \times 10^4 \pm 0.7\%$	$800 \pm 4\%$
Cell 5 Furnace	1.5×10^3 (MDA)	1.1×10^3 (MDA)	220 (MDA)

Table 4-1: Counts in Major Pu-238 Photopeaks for HPGe Measurements. The cell interiors values are the sum of the counts in the sequence of measurements taken beneath that cell in the vertical detector orientation. *The count time for the Cell 1 North Furnace was 480 seconds, while all other count times were 120 seconds.

4.2 Detector Efficiency

The uncollimated detector efficiency for the HPGe was measured using two point sources: a Ho-166m source (IPL-1278-38) and a mixture of Eu-152, Eu-154, and Eu-155 (EZ-1480-93-10 and EZ-1480-93-9). The europium isotope blend was produced at SRNL from two liquid standards that were mixed and dried on a planchet. The sources were located 38.1 cm from the face of the detector directly on its central axis. The efficiency curve for this detector was determined using Canberra's Genie 2000 software [13] and is shown in Figure 4-1. The uncollimated detector efficiency for a point source at 38.1 cm from the face of the detector and associated uncertainties arising from curve fitting and source activity are found in Table 4-2.

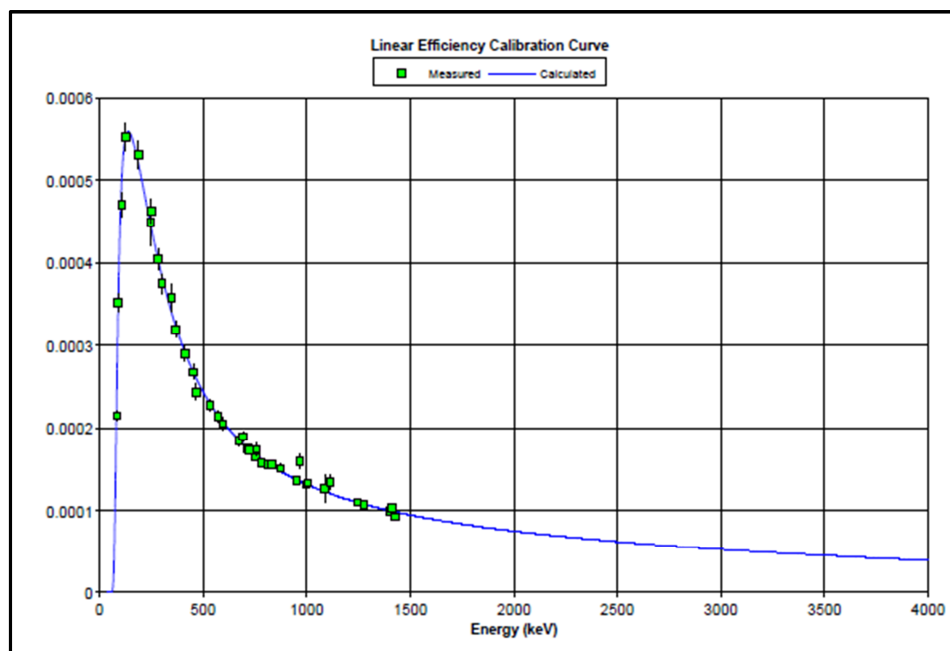


Figure 4-1: Point Source Efficiency for HPGe Detector located 38.1 cm from Ho-166m, Eu-152, Eu-154, and Eu-155 gamma-ray sources.

The collimator used for the assay was fabricated just before the measurements. Calibration data were not taken prior to the assay with the collimator because of time constraints. During the assay, the collimator was contaminated and was unavailable for calibration measurements. A second identical collimator was fabricated and efficiency calibrations were performed with and without the collimator using a Ho-166m point source. The detector efficiency had degraded slightly in the interim, thus the original uncollimated detector efficiency was used for analysis modified by a correction factor to account for the collimator

effect. This energy-dependent correction factor was determined by fitting the ratio of the count rates in the collimated to uncollimated photopeaks to a logarithmic function. Table 4-2 contains the collimation adjustment factor and the effective collimated efficiency to a point source 38.1 cm from the detector face. Figure 4-2 shows the data points and the resultant fit given by the following function, where the gamma energy (E) is in keV, $a = 0.040 \pm 0.005$, and $b = 0.69 \pm 0.03$:

$$f_{col} = a \ln(E) + b.$$

Energy (keV)	Uncollimated Efficiency	Fit Error (%)	Source Activity Error (%)	f_{col}	Collimated Efficiency
99.85	4.3×10^{-4}	1.8	3.0	$0.88 \pm 4\%$	$3.8 \times 10^{-4} \pm 6\%$
152.7	5.9×10^{-4}	1.8	3.0	$0.89 \pm 4\%$	$5.3 \times 10^{-4} \pm 6\%$
766.4	1.66×10^{-4}	0.8	3.0	$0.96 \pm 6\%$	$1.6 \times 10^{-4} \pm 6\%$

Table 4-2: Point Source Efficiencies and Associated Uncertainties.

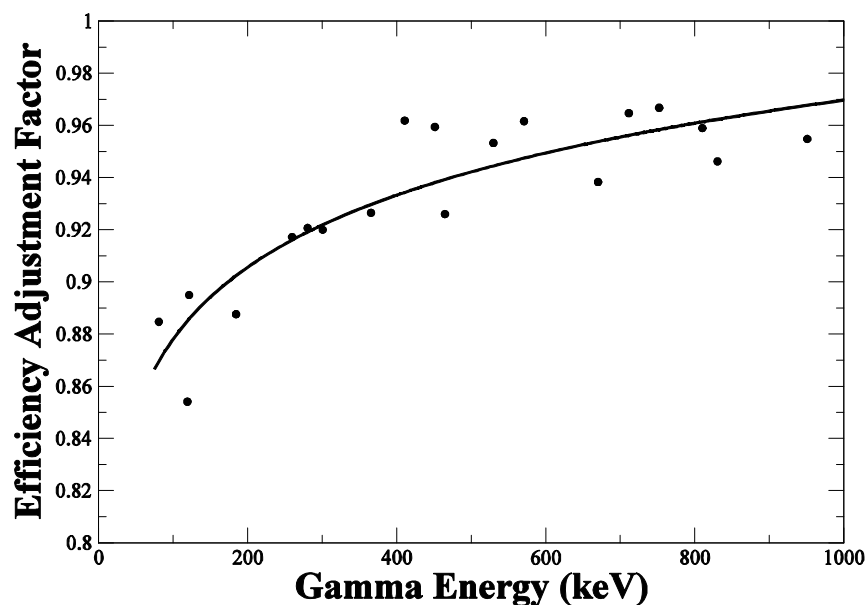


Figure 4-2: Effect of Collimator of HPGe Detector Efficiency. Data points are the ratio of count rates in photopeaks from Ho-166m with the collimator to the count rates without the collimator. The solid line is a curve fit to the data used to estimate the magnitude of this effect at the three assay energies.

4.3 Solid Angle and Attenuation Corrections

The overall detector efficiency (ε) defined as the probability that a gamma-ray emitted by the Pu-238 is detected by the HPGe detector may be expressed as three independent parameters as follows:

$$\varepsilon = \varepsilon_0 \alpha \Omega \quad \text{Equation 4-2}$$

where, ε_0 is the energy-dependent intrinsic detector efficiency (the probability that a photon that hits the detector is counted in the photopeak), α is the energy-dependent attenuation coefficient (the fraction of photons emitted in the direction of the detector that arrive unscattered), and Ω is the average solid angle of the detector relative to the source distribution (the fraction of photons emitted by the source emitted in the direction of the detector).

The intrinsic detector efficiency is the same for the point source calibration and the assay measurements. The MCNP calculations detailed in Section 3 provide the product of the attenuation coefficient and the solid angle, which will be defined as ϕ_{MCNP} , the photon flux (cm^{-2}) at the detector face normalized per source photon (at the energy used for the analysis) from the source distributions modeled. This same parameter may be defined for the point source calibration configuration as ϕ_p , the photon flux (cm^{-2}) at the detector face normalized per source photon from a point source located 38.1 cm from the face of the detector. Thus the detector efficiency for the assay geometry is given as follows:

$$\varepsilon = \varepsilon_p \left(\frac{\phi_{MCNP}}{\phi_p} \right) \quad \text{Equation 4-3.}$$

Making this substitution into $M_{238Pu} = \frac{N_{net}}{S_{238Pu} \cdot BR_\gamma \cdot \varepsilon \cdot t}$ Equation 4-1, the equation used to calculate the

holdup mass of Pu-238 in the cells becomes:

$$M_{238Pu} = \frac{N_{net} \cdot \phi_p}{S_{238Pu} \cdot BR_\gamma \cdot \varepsilon_p \cdot \phi_{MCNP} \cdot t} \quad \text{Equation 4-4}$$

Since attenuation is negligible for the point source calibration geometry, the parameter, ϕ_p , and its uncertainty may be calculated as follows:

$$\phi_p = \frac{1}{4\pi r^2} \text{ Equation 4-5 and } \partial\phi_p = \frac{\partial r}{2\pi r^3} \text{ Equation 4-6.}$$

Inserting $r = 38.1 \pm 0.5$ cm into Equations 4.5 and 4.6, $\phi_p = 5.48 \times 10^{-5} \text{ cm}^{-2} \pm 2.6\%$.

After examining preliminary assay results using Equation 4-4, it appeared that the attenuation had been overestimated by the models, nearly across the board. The assay mass obtained using the 99.85 keV gamma-ray was considerably larger than the mass obtained using the 152.7 keV gamma-ray which was larger than the 766.4 keV assay mass. The assay masses were adjusted to account for this by effectively removing a small amount of the attenuating material from the models. The assay mass for each energy was modified by the following function:

$$M_{^{238}\text{Pu}} = M_{^{238}\text{Pu}}^0 \exp(-\mu_E \rho d) \text{ Equation 4-7}$$

where, μ_E is the mass attenuation coefficient (cm^2/g) [15], ρ is the density of the attenuating material, and d is the thickness removed from the model. Each energy had its own mass attenuation coefficient, but the density and thickness of the attenuating layer was the same across the three energies. A common thickness was calculated that minimized the variance between the three assay masses. For the cell interior measurements, steel was the natural choice for the material. The effective reduction in steel thickness was less than 0.5 cm for the worst case (HML in Cell 1) and more typically on the order of 1-2 mm. This is quite reasonable since the girders and material in the cells were rather crudely approximated. This treatment was also applied to the furnaces in Cell 1. Here the choice of material is not as clear, either tungsten, steel, or aluminum oxide. The procedure was attempted with all three material, however only tungsten gave reasonable results (e.g. more than 3 cm of steel would have been removed). The amount of tungsten removed from the model was less than 1 mm for all cases. This treatment was not applied to the coolers or the Cell 5 furnace as the assay of these objects gave MDAs for at least one energy.

4.4 Cross Talk

Since the detector used for the assay measurements was highly collimated, cross talk between cells or between furnaces and cells was a relatively small effect. Therefore, it was treated as a source of uncertainty rather than being corrected in the assay mass. The relative uncertainty induced by cross talk was estimated using the following equations:

$$\sigma_{CT} = \sum_i \frac{M_i \epsilon_i^{CT}}{M \epsilon} \quad \text{Equation 4-8}$$

where, the summation runs over neighboring cells or other sources of cross talk. The numerator is proportional to the cross talk count rate and the denominator to the count rate from the mass distribution being assayed.

5.0 Assay Results

The mass of Pu-238 for each object assayed at the three gamma-ray energies may be found in Table 5-1 along with the associated uncertainties. The breakdown of the contributions of the various sources of uncertainty for the 99.85 keV, 152.7 keV, and 766.4 keV analyses may be found in Tables 5-2, 5-3, and 5-4, respectively.

	Assay Masses (g)		
	99.85 keV	152.7 keV	766.4 keV
Cell 1 Interior	120 ± 10 (8%)	107 ± 9 (8%)	120 ± 15 (13%)
Cell 1 North Furnace	15 ± 9 (60%)	30 ± 12 (40%)	13 ± 8 (60%)
Cell 1 South Furnace	41 ± 21 (50%)	56 ± 24 (44%)	36 ± 22 (60%)
Cell 1 Cooler	34.7 (MDA)	10.7 (MDA)	25.6 (MDA)
Cell 2 Interior	39 ± 6 (14%)	32 ± 4 (14%)	41 ± 8 (19%)
Cell 2 North Cooler	34 ± 5 (13%)	9.9 ± 1.4 (14%)	7.7 (MDA)
Cell 2 South Cooler	N/A	N/A	12.7 (MDA)
Cell 3 Interior	2.8 ± 0.6 (23%)	2.1 ± 0.6 (26%)	3.0 ± 1.2 (40%)
Cell 3 Cooler	17.1 (MDA)	7.3 (MDA)	9.5 (MDA)
Cell 4 Interior	10.3 ± 1.1 (10%)	8.8 ± 0.9 (10%)	10.6 ± 1.5 (15%)
Cell 4 Cooler	90.9 (MDA)	24.4 (MDA)	22.4 (MDA)
Cell 5 Interior	9.1 ± 0.8 (9%)	8.2 ± 0.7 (9%)	9.2 ± 1.4 (15%)
Cell 5 Cooler	91.5 (MDA)	22.9 (MDA)	25.0 (MDA)
Cell 5 Furnace	702.9 (MDA)	16.2 (MDA)	12.4 (MDA)

Table 5-1: Assay Results for the Three Gamma-Ray Energies.

	Cell 1 Interior	Cell 2 Interior	Cell 3 Interior	Cell 4 Interior	Cell 5 Interior	Cell 1 North Furnace	Cell 1 South Furnace	Cell 2 North Cooler
Source Location	1.2%	1.1%	0.9%	0.8%	2.2%	60%	43%	N/A
Sample Holder Density	N/A	N/A	N/A	N/A	N/A	8%	12%	N/A
Alumina Bubble Density	N/A	N/A	N/A	N/A	N/A	14%	20%	N/A
Specific Activity	0.1%	0.1%	0.1%	0.1%	0.1%	0.1%	0.1%	0.1%
Branching Ratio	1.1%	1.1%	1.1%	1.1%	1.1%	1.1%	1.1%	1.1%
Point Source Efficiency	3.5%	3.5%	3.5%	3.5%	3.5%	3.5%	3.5%	3.5%
Point Source Flux	2.6%	2.6%	2.6%	2.6%	2.6%	2.6%	2.6%	2.6%
Collimation	4.3%	4.3%	4.3%	4.3%	4.3%	4.3%	4.3%	4.3%
Attenuation	5.3%	11%	14%	8%	5%	9%	9%	N/A
Counting Statistics	0.1%	0.2%	0.7%	0.3%	0.4%	0.7%	0.7%	5.4%
MCNP Statistics	0.4%	0.4%	0.4%	0.4%	0.4%	3%	2.2%	2.2%
Cross Talk	0.02%	6%	18%	1.2%	3%	0%	0%	0%
Net	8%	14%	23%	10%	9%	60%	50%	13%

Table 5-2: Sources of Uncertainty for 99.85 keV Analysis.

	Cell 1 Interior	Cell 2 Interior	Cell 3 Interior	Cell 4 Interior	Cell 5 Interior	Cell 1 North Furnace	Cell 1 South Furnace	Cell 2 North Cooler
Source Location	1.3%	0.8%	0.7%	0.7%	1.6%	24%	27%	N/A
Sample Holder Density	N/A	N/A	N/A	N/A	N/A	18%	19%	N/A
Alumina Bubble Density	N/A	N/A	N/A	N/A	N/A	26%	27%	N/A
Specific Activity	0.1%	0.1%	0.1%	0.1%	0.1%	0.1%	0.1%	0.1%
Branching Ratio	0.8%	0.8%	0.8%	0.8%	0.8%	0.8%	0.8%	0.8%
Point Source Efficiency	3.5%	3.5%	3.5%	3.5%	3.5%	3.5%	3.5%	3.5%
Point Source Flux	2.6%	2.6%	2.6%	2.6%	2.6%	2.6%	2.6%	2.6%
Collimation	4.4%	4.4%	4.4%	4.4%	4.4%	4.4%	4.4%	4.4%
Attenuation	5.3%	11%	14%	8%	5%	9%	9%	N/A
Counting Statistics	0.1%	0.2%	1.2%	0.4%	0.6%	0.9%	0.9%	7%
MCNP Statistics	0.2%	0.2%	0.2%	0.2%	0.2%	0.4%	0.2%	0.7%
Cross Talk	0.04%	6%	21%	1.2%	3.5%	0%	0%	N/A
Net	8%	14%	26%	10%	9%	40%	44%	14%

Table 5-3: Sources of Uncertainty for 152.7 keV Analysis.

	Cell 1 Interior	Cell 2 Interior	Cell 3 Interior	Cell 4 Interior	Cell 5 Interior	Cell 1 North Furnace	Cell 1 South Furnace
Source Location	1.2%	1.3%	0.9%	0.9%	1.5%	53%	54%
Sample Holder Density	N/A	N/A	N/A	N/A	N/A	11%	11%
Alumina Bubble Density	N/A	N/A	N/A	N/A	N/A	16%	16%
Specific Activity	0.1%	0.1%	0.1%	0.1%	0.1%	0.1%	0.1%
Branching Ratio	9.1%	9.1%	9.1%	9.1%	9.1%	9.1%	9.1%
Point Source Efficiency	3.1%	3.1%	3.1%	3.1%	3.1%	3.1%	3.1%
Point Source Flux	2.6%	2.6%	2.6%	2.6%	2.6%	2.6%	2.6%
Collimation	4.7%	4.7%	4.7%	4.7%	4.7%	4.7%	4.7%
Attenuation	5.3%	11%	14%	8%	5%	9%	9%
Counting Statistics	1.3%	2.5%	14%	4.5%	7%	6%	4%
MCNP Statistics	0.2%	0.2%	0.2%	0.2%	0.2%	0.2%	0.1%
Cross Talk	3.4%	10%	34%	1.6%	5%	0%	0%
Net	13%	19%	40%	15%	15%	60%	60%

Table 5-4: Sources of Uncertainty for 766.4 keV Analysis.

The assay results for each of the three energies considered are essentially completely independent measurements (excluding the attenuation correction procedure). The final assay result for the cell interiors and the Cell 1 furnaces were based on the weighted mean of the result for each of the three energies, where the weighting factor is based on the uncertainty of the measurements.

Thus the final assay mass and uncertainty are given by the following expressions:

$$\bar{M} = \frac{\sum_{i=1}^3 \frac{M_{E_i}}{\partial M_{E_i}^2}}{\sum_{i=1}^3 \frac{1}{\partial M_{E_i}^2}} \quad \text{Equation 5-1} \quad \text{and} \quad \partial \bar{M} = \left(\sum_{i=1}^3 \frac{1}{\partial M_{E_i}^2} \right)^{-\frac{1}{2}} \quad \text{Equation 5-2}$$

When analysis of all three gamma-ray energies resulted in MDAs, the lowest MDA for the three energies analyzed was reported. The final assay masses for the East Cell Line from the current assay are reported in Table 5-5 along with the previous results from the 2006 scoping assay [3]. The cooler in Cell 5 was not assayed with the HPGe detector, because of geometric constraints. The MDAs reported for this cooler are based on the LaBr scoping measurements. Summing the assay results and treating MDAs as $M_{238\text{Pu}} = 0 \pm \text{MDA}$, the total holdup in the East Cell Line was 240 ± 40 grams. This is 100 grams or 0.55σ lower than the 2006 scoping assay results though the previous results did not account for holdup in the furnaces or coolers. However, the current assay results are in agreement with the 2006 scoping assay results due to the large uncertainty associated with the 2006 scoping assays. The current assay results support the conclusion that the 2006 results bound the Pu-238 mass in Cells 1-5. A conservative bounding upper limit to the cell interior assay results was obtained by performing calculation with the assumption that all the Pu-238 is located on the ceiling of the cells. The results of these calculations may be found in Table 5-6. The accuracy of the assay results may be improved further with additional knowledge of the source distribution. In-cell measurements are planned that should provide this information. These assay results do not include the wing-cabinets in the East Maintenance area or the

transfer line between the East and West Cell Lines. Measurements of these areas are planned for 2016 or 2017.

	Current Assay Mass (g)	2006 Scoping Assay Mass (g) [3]
Cell 1 Interior	114 ± 6 (5%)	264.3 ± 166.5 (63%)
Cell 1 North Furnace	17 ± 5 (31%)	Not Measured
Cell 1 South Furnace	43 ± 13 (28%)	Not Measured
Cell 1 Cooler	10.7 (MDA)	Not Measured
Cell 2 Interior	36 ± 3 (9%)	59.7 ± 43.6 (73%)
Cell 2 North Cooler	11.9 ± 1.3 (11%)	Not Measured
Cell 2 South Cooler	12.7 (MDA)	Not Measured
Cell 3 Interior	2.5 ± 0.4 (16%)	2.17 ± 1.45 (67%)
Cell 3 Cooler	7.3 (MDA)	Not Measured
Cell 4 Interior	9.6 ± 0.6 (7%)	9.82 ± 7.27 (74%)
Cell 4 Cooler	22.4 (MDA)	Not Measured
Cell 5 Interior	8.7 ± 0.5 (6%)	4.58 ± 3.25 (71%)
Cell 5 Cooler	22.9 (MDA)	Not Measured
Cell 5 Furnace	12.4 (MDA)	Not Measured
Total East Cell Line	240 ± 40 (17%)	340 ± 170 (50%)

Table 5-5: Current Assay Results compared with 2006 Scoping Measurements [3].

Cell	Mass (g)
Cell 1	156.3
Cell 2	58.9
Cell 3	3.9
Cell 4	13.9
Cell 5	12.7

Table 5-6: Conservative Upper Limit for Cell Interior Assays Assuming Pu-238 Distribution on Cell Ceilings.

6.0 References

- [1] “Report of an Investigation into the Deterioration of the Plutonium Fuel Forms Fabrication Facility (PuFF) at the DOE Savannah River Site” Department of Energy – Nuclear Safety, DOE/NS-0002P, (1991)
- [2] X-5 Monte-Carlo Team. “MCNP – A General N-Particle Transport Code, Version 5, Volume 1: Overview and Theory” Los Alamos National Laboratory. LA-UR-03-1987. (2003)
- [3] D.W. Roberts. “FAMS Hold-Up Measurements for PuFF Process Cells” Savannah River Site. N-CLC-F-00796. (2006)
- [4] “Savannah River Plant Building 235-F F.F Cell Line Plan Cells 1 & 2 Equipment Arrangement Process” Savannah River Site, Drawing W448043, (1974)
- [5] “Savannah River Plant Building 235-F Cell Line Plan Cell 3, 4, & 5 Equipment Arrangement Process” Savannah River Site, Drawing W447942, (1974)
- [6] “Basis for Interim Operation for Building 235-F.” Savannah River Site, U-BIO-F-00003 Revision 1, (2014)
- [7] J.C. Musall and Dennis McKaskill. Private Communication. (2014)
- [8] B. Rooney, S. Garner, and P. Felsher. PeakEasy 4.51. Los Alamos National Laboratory. LA-CC-13-040. (2013)
- [9] L.A. Currie. “Limits for Qualitative Detection and Quantitative Determination: Application to Radiochemistry.” Anal. Chem. 40, 586-593 (1968)
- [10] J.K Blankenship and J.C. Musall. “Deactivation Project Plan Plutonium Fuel Form Facility Building 235-F, Metallurgical Building” V-PMP-F00083, Savannah River Site, (2013)

- [11] R.J. McConn, Jr., *et al.* “Compendium of Material Composition Data for Radiation Transport Modeling.” PIET-43741-TM-963, PNNL-15870 Rev.1, Pacific Northwest National Laboratory, (2011)
- [12] E. Brown and J.K Tuli. “Nuclear Data Sheets for A=234.” Nuclear Data Sheets 108, 681 (2007)
- [13] “Genie 2000 Spectroscopy Software: Operations Manual.” Canberra Industries, Inc. (2012)
- [14] J.H. Hubbell and S.M. Seltzer, Tables of X-Ray Mass Attenuation Coefficients and Mass Energy-Absorption Coefficients (version 1.4). [Online] (2004).

Appendix A. Detector Locations for Cell Interior Assays

The table below gives the x- and y-coordinates for the central detector locations during the measurements used for the cell interior assay analyses. The coordinates are referenced relative to an origin located at the northwest interior corner of Cell 1. All measurements were taken at the same height, where the face of the detector was 104.14 cm beneath the bottom surface of the cell floors.

Reference Number	X-Coordinate (cm)	Y-Coordinate (cm)
Cell 1		
1	23.77	49.53
2	19.91	74.30
3	19.91	106.68
4	77.79	40.96
5	72.28	66.68
6	105.35	40.96
7	105.35	77.79
8	105.35	111.44
9	149.45	111.44
10	164.15	77.79
11	183.75	44.45
12	193.55	77.79
13	193.55	111.44
14	235.20	111.44
15	237.65	77.79
16	235.20	43.82
17	298.29	43.82
18	298.29	77.79
19	298.29	111.44
20	333.81	77.79
21	333.81	40.96
22	369.95	40.96
23	369.95	77.79
24	367.01	111.44
25	426.30	111.44
26	432.12	77.79
27	457.54	111.44
28	474.69	88.27
29	479.59	40.96
Cell 2		
1	518.32	116.52
2	558.48	111.44
3	558.48	75.25
4	595.95	40.96
5	625.79	118.11

6	657.54	116.52
7	668.34	81.28
8	695.65	43.82
9	695.65	76.20
10	710.88	111.44
Cell 3		
1	759.14	78.74
2	742.95	40.96
3	795.66	80.01
4	795.66	111.44
5	854.08	111.44
6	854.08	77.15
7	852.49	40.96
8	905.51	40.96
9	905.51	76.20
10	905.51	111.44
Cell 4		
1	974.41	111.44
2	971.55	76.20
3	977.27	40.96
4	1034.42	40.96
5	1034.42	80.01
6	1034.42	111.44
7	1083.95	111.44
8	1083.95	76.20
9	1084.26	40.96
10	1131.25	40.96
11	1141.10	88.58
12	1158.24	111.44
13	1210.31	116.84
Cell 5		
1	1241.43	40.96
2	1229.68	72.39
3	1260.79	111.44
4	1261.43	71.44
5	1304.29	76.20
6	1330.01	40.96
7	1389.70	105.73
8	1402.40	77.72

Table A-6-1: Detector Locations for Cell Interior Assays


```
C DIRECTIONAL BIASING
C
C A FACTOR OF 3 MUST BE INCLUDED SINCE THE SOURCE IS SPLIT BETWEEN
C 3 ENERGIES
C
C THIS MEANS FLUX RESULTS MUST BE MULTIPLIED BY 0.15
C
C CELLS ARE FILLED WITH STAINLESS STEEL MATERIAL UP TO 30 cm IN ALL
C CELLS. DENSITY OF THIS MATERIAL IS BASED ON WEIGHT ESTIMATES FROM
C CELL INVENTORIES.
C
C MID RANGE ESTIMATES
C
C CELL MATERIAL FILL DENSITY (g/cm^3)
C
C 1 0.083
C 2 0.044
C 3 0.020
C 4 0.026
C 5 0.083
C
C SOURCE UNIFORMLY DISTRIBUTED IN MATERIAL FILL (ONE CELL AT A TIME)
C
C @@@@ CELL_NUM = 16 26 36 46 56
C
C MCNP_PSTUDY IS USED TO RUN A BATCH FOR THE FIVE CELLS (1,2,3,4,5)
C
C CCCCCCCCCCCCCCCCCCCCCCCCCCCCCCCCCCCCCCCCCCCCCCCCCCCCCCCCCCCCCCCC
C
C CELL CARDS
C
C CCCCCCCCCCCCCCCCCCCCCCCCCCCCCCCCCCCCCCCCCCCCCCCCCCCCCCCCCCCCCCCC
C
C CELL 1
C
10 800 -0.001205 7 -1 9 IMP:P=1 $ INTERIOR
11 100 -7.92 -2 1 IMP:P=1 $ WALLS
12 200 -0.321 -3 4 5 #178 IMP:P=1 $ GIRDERS
13 800 -0.001205 -4 #76 IMP:P=1 $ GIRDER CUTOUT 1
14 800 -0.001205 -5 #77 IMP:P=1 $ GIRDER CUTOUT 2
15 800 -0.001205 -6 69 IMP:P=1 $ CELL GAP
16 100 -0.083 -1 -7 IMP:P=1 $ MATERIAL FILL
17 400 -0.02 -8 IMP:P=1 $ HEPA
18 100 -7.92 8 -9 IMP:P=1 $ HEPA BOX
C
C CELL 2
C
20 800 -0.001205 17 -11 19 IMP:P=1 $ INTERIOR
21 100 -7.92 -12 11 IMP:P=1 $ WALLS
22 200 -0.393 -13 98 #190 IMP:P=1 $ GIRDERS
25 800 -0.001205 -16 69 IMP:P=1 $ CELL GAP
26 100 -0.044 -11 -17 IMP:P=1 $ MATERIAL FILL
27 400 -0.02 -18 IMP:P=1 $ HEPA
```

28 100 -7.92 18 -19 IMP:P=1 \$ HEPA BOX
C
C CELL 3
C
30 800 -0.001205 27 -21 29 IMP:P=1 \$ INTERIOR
31 100 -7.92 -22 21 IMP:P=1 \$ WALLS
32 200 -0.315 -23 IMP:P=1 \$ GIRDERS
33 700 -1.0 -25 IMP:P=1 \$ COOLER INTERIOR
34 100 -7.92 -24 25 IMP:P=1 \$ COOLER WALLS
35 800 -0.001205 -26 69 IMP:P=1 \$ CELL GAP
36 100 -0.020 -21 -27 IMP:P=1 \$ MATERIAL FILL
37 400 -0.02 -28 IMP:P=1 \$ HEPA
38 100 -7.92 28 -29 IMP:P=1 \$ HEPA BOX
C
C CELL 4
C
40 800 -0.001205 37 -31 39 IMP:P=1 \$ INTERIOR
41 100 -7.92 -32 31 IMP:P=1 \$ WALLS
42 200 -0.286 -33 IMP:P=1 \$ GIRDERS
43 700 -1.0 -35 IMP:P=1 \$ COOLER INTERIOR
44 100 -7.92 -34 35 IMP:P=1 \$ COOLER WALLS
45 800 -0.001205 -36 69 IMP:P=1 \$ CELL GAP
46 100 -0.026 -31 -37 IMP:P=1 \$ MATERIAL FILL
47 400 -0.02 -38 IMP:P=1 \$ HEPA
48 100 -7.92 38 -39 IMP:P=1 \$ HEPA BOX
C
C CELL 5
C
50 800 -0.001205 47 -41 49 IMP:P=1 \$ INTERIOR
51 100 -7.92 -42 41 IMP:P=1 \$ WALLS
52 200 -0.150 -43 46 IMP:P=1 \$ GIRDERS
53 700 -1.0 -45 IMP:P=1 \$ COOLER INTERIOR
54 100 -7.92 -44 45 IMP:P=1 \$ COOLER WALLS
55 800 -0.001205 -46 #78 IMP:P=1 \$ FURNACE CUTOOT
56 100 -0.083 -41 -47 IMP:P=1 \$ MATERIAL FILL
57 400 -0.02 -48 IMP:P=1 \$ HEPA
58 100 -7.92 48 -49 IMP:P=1 \$ HEPA BOX
C
C FURNACES
C
60 100 -8.0 -51 52 U=1 IMP:P=1 \$ SKIN
61 700 -1.0 -52 65 U=1 IMP:P=1 \$ SHELL GAP (WATER FILLED)
62 100 -8.0 -53 54 U=1 IMP:P=1 \$ INNER SHELL
63 500 -0.76 -54 55 56 U=1 IMP:P=1 \$ ALUMINA BUBBLES
64 600 -8.06 -55 56 U=1 IMP:P=1 \$ HEATING ELEMENT
65 500 -3.85 -56 57 U=1 IMP:P=1 \$ HEATER TUBE
66 800 -0.001205 -57 58 U=1 IMP:P=1 \$ AIR GAP
67 500 -3.85 -58 59 U=1 IMP:P=1 \$ WORK TUBE
68 500 -0.84 -62 U=1 IMP:P=1 \$ SAMPLE HOLDER
69 800 -0.001205 62 -59 60 -63 U=1 IMP:P=1 \$ VOID SPACE 1
70 800 -0.001205 -61 U=1 IMP:P=1 \$ INSIDE SAMP. SUPP. TUBE
71 500 -3.85 -60 61 U=1 IMP:P=1 \$ SAMP. SUPP. TUBE
72 500 -3.85 60 -59 63 -64 U=1 IMP:P=1 \$ WORK TUBE INSULATION

```

73 800 -0.001205 60 -59 64 U=1 IMP:P=1 $ VOID SPACE 2
74 100 -8.0 -65 66 U=1 IMP:P=1 $ MIDDLE SHELL
75 800 -0.001205 -66 53 U=1 IMP:P=1 $ SHELL GAP (AIR FILLED)
76 0 -67 FILL=1 TRCL=1 IMP:P=1 $ FURNACE 1 CELL 1
77 0 -67 FILL=1 TRCL=2 IMP:P=1 $ FURNACE 2 CELL 1
78 0 -67 FILL=1 TRCL=3 IMP:P=1 $ FURNACE CELL 5
79 800 -0.001205 51 U=1 IMP:P=1 $ OUTSIDE FURNACE
C
C COLLIMATOR
C
80 0 (-73:-70) 77 U=2 IMP:P=1 $ COLLIMATOR VOID
81 100 -7.92 -71 70 U=2 IMP:P=1 $ STEEL COLLIMATOR TUBE
82 900 -9.6 -72 71 73 U=2 IMP:P=1 $ TUNGSTEN SHOT
83 0 -76 FILL=2 TRCL=4 IMP:P=1 $ CELL 1 COLLIMATOR 2
84 0 -76 FILL=2 TRCL=5 IMP:P=1 $ CELL 1 COLLIMATOR 3
85 0 -76 FILL=2 TRCL=6 IMP:P=1 $ CELL 1 COLLIMATOR 4
86 0 -76 FILL=2 TRCL=7 IMP:P=1 $ CELL 1 COLLIMATOR 5
87 0 -76 FILL=2 TRCL=8 IMP:P=1 $ CELL 1 COLLIMATOR 6
88 0 -76 FILL=2 TRCL=9 IMP:P=1 $ CELL 1 COLLIMATOR 8
89 0 -76 FILL=2 TRCL=10 IMP:P=1 $ CELL 1 COLLIMATOR 9
90 0 -76 FILL=2 TRCL=11 IMP:P=1 $ CELL 1 COLLIMATOR 10
91 0 -76 FILL=2 TRCL=12 IMP:P=1 $ CELL 1 COLLIMATOR 11
92 0 -76 FILL=2 TRCL=13 IMP:P=1 $ CELL 1 COLLIMATOR 12
93 0 -76 FILL=2 TRCL=14 IMP:P=1 $ CELL 1 COLLIMATOR 13
94 0 -76 FILL=2 TRCL=15 IMP:P=1 $ CELL 1 COLLIMATOR 14
95 0 -76 FILL=2 TRCL=16 IMP:P=1 $ CELL 1 COLLIMATOR 15
96 0 -76 FILL=2 TRCL=17 IMP:P=1 $ CELL 1 COLLIMATOR 16
97 0 -76 FILL=2 TRCL=18 IMP:P=1 $ CELL 1 COLLIMATOR 17
98 0 -76 FILL=2 TRCL=19 IMP:P=1 $ CELL 1 COLLIMATOR 18
99 0 -76 FILL=2 TRCL=20 IMP:P=1 $ CELL 1 COLLIMATOR 19
100 0 -76 FILL=2 TRCL=21 IMP:P=1 $ CELL 1 COLLIMATOR 20
101 0 -76 FILL=2 TRCL=22 IMP:P=1 $ CELL 1 COLLIMATOR 21
102 0 -76 FILL=2 TRCL=23 IMP:P=1 $ CELL 1 COLLIMATOR 22
103 0 -76 FILL=2 TRCL=24 IMP:P=1 $ CELL 1 COLLIMATOR 23
104 0 -76 FILL=2 TRCL=25 IMP:P=1 $ CELL 1 COLLIMATOR 24
105 0 -76 FILL=2 TRCL=26 IMP:P=1 $ CELL 1 COLLIMATOR 25
106 0 -76 FILL=2 TRCL=27 IMP:P=1 $ CELL 1 COLLIMATOR 26
107 0 -76 FILL=2 TRCL=28 IMP:P=1 $ CELL 1 COLLIMATOR 27
108 0 -76 FILL=2 TRCL=29 IMP:P=1 $ CELL 1 COLLIMATOR 28
109 0 -76 FILL=2 TRCL=30 IMP:P=1 $ CELL 1 COLLIMATOR 29
110 0 -76 FILL=2 TRCL=31 IMP:P=1 $ CELL 1 COLLIMATOR 30
111 0 -76 FILL=2 TRCL=32 IMP:P=1 $ CELL 1 COLLIMATOR 31
112 0 -76 FILL=2 TRCL=33 IMP:P=1 $ CELL 2 COLLIMATOR 32
113 0 -76 FILL=2 TRCL=34 IMP:P=1 $ CELL 2 COLLIMATOR 33
114 0 -76 FILL=2 TRCL=35 IMP:P=1 $ CELL 2 COLLIMATOR 34
115 0 -76 FILL=2 TRCL=36 IMP:P=1 $ CELL 2 COLLIMATOR 35
116 0 -76 FILL=2 TRCL=37 IMP:P=1 $ CELL 2 COLLIMATOR 36
117 0 -76 FILL=2 TRCL=38 IMP:P=1 $ CELL 2 COLLIMATOR 37
118 0 -76 FILL=2 TRCL=39 IMP:P=1 $ CELL 2 COLLIMATOR 38
119 0 -76 FILL=2 TRCL=40 IMP:P=1 $ CELL 2 COLLIMATOR 39
120 0 -76 FILL=2 TRCL=41 IMP:P=1 $ CELL 2 COLLIMATOR 40
121 0 -76 FILL=2 TRCL=42 IMP:P=1 $ CELL 2 COLLIMATOR 41
122 0 -76 FILL=2 TRCL=43 IMP:P=1 $ CELL 3 COLLIMATOR 1

```

123 0 -76 FILL=2 TRCL=44 IMP:P=1 \$ CELL 3 COLLIMATOR 2
124 0 -76 FILL=2 TRCL=45 IMP:P=1 \$ CELL 3 COLLIMATOR 3
125 0 -76 FILL=2 TRCL=46 IMP:P=1 \$ CELL 3 COLLIMATOR 4
126 0 -76 FILL=2 TRCL=47 IMP:P=1 \$ CELL 3 COLLIMATOR 5
127 0 -76 FILL=2 TRCL=48 IMP:P=1 \$ CELL 3 COLLIMATOR 6
128 0 -76 FILL=2 TRCL=49 IMP:P=1 \$ CELL 3 COLLIMATOR 7
129 0 -76 FILL=2 TRCL=50 IMP:P=1 \$ CELL 3 COLLIMATOR 8
130 0 -76 FILL=2 TRCL=51 IMP:P=1 \$ CELL 3 COLLIMATOR 9
131 0 -76 FILL=2 TRCL=52 IMP:P=1 \$ CELL 3 COLLIMATOR 10
132 0 -76 FILL=2 TRCL=53 IMP:P=1 \$ CELL 4 COLLIMATOR 11
133 0 -76 FILL=2 TRCL=54 IMP:P=1 \$ CELL 4 COLLIMATOR 12
134 0 -76 FILL=2 TRCL=55 IMP:P=1 \$ CELL 4 COLLIMATOR 13
135 0 -76 FILL=2 TRCL=56 IMP:P=1 \$ CELL 4 COLLIMATOR 14
136 0 -76 FILL=2 TRCL=57 IMP:P=1 \$ CELL 4 COLLIMATOR 15
137 0 -76 FILL=2 TRCL=58 IMP:P=1 \$ CELL 4 COLLIMATOR 16
138 0 -76 FILL=2 TRCL=59 IMP:P=1 \$ CELL 4 COLLIMATOR 17
139 0 -76 FILL=2 TRCL=60 IMP:P=1 \$ CELL 4 COLLIMATOR 18
140 0 -76 FILL=2 TRCL=61 IMP:P=1 \$ CELL 4 COLLIMATOR 19
141 0 -76 FILL=2 TRCL=62 IMP:P=1 \$ CELL 4 COLLIMATOR 20
142 0 -76 FILL=2 TRCL=63 IMP:P=1 \$ CELL 4 COLLIMATOR 21
143 0 -76 FILL=2 TRCL=64 IMP:P=1 \$ CELL 4 COLLIMATOR 22
144 0 -76 FILL=2 TRCL=65 IMP:P=1 \$ CELL 4 COLLIMATOR 23
145 0 -76 FILL=2 TRCL=66 IMP:P=1 \$ CELL 5 COLLIMATOR 24
146 0 -76 FILL=2 TRCL=67 IMP:P=1 \$ CELL 5 COLLIMATOR 25
147 0 -76 FILL=2 TRCL=68 IMP:P=1 \$ CELL 5 COLLIMATOR 26
148 0 -76 FILL=2 TRCL=69 IMP:P=1 \$ CELL 5 COLLIMATOR 27
149 0 -76 FILL=2 TRCL=70 IMP:P=1 \$ CELL 5 COLLIMATOR 28
150 0 -76 FILL=2 TRCL=71 IMP:P=1 \$ CELL 5 COLLIMATOR 29
151 0 -76 FILL=2 TRCL=72 IMP:P=1 \$ CELL 5 COLLIMATOR 30
152 0 -76 FILL=2 TRCL=73 IMP:P=1 \$ CELL 5 COLLIMATOR 31
153 800 -0.001205 72 U=2 IMP:P=1 \$ OUTSIDE COLLIMATOR
154 0 -77 U=2 IMP:P=1 \$ DETECTION REGION
C
C CELL 1 COOLER
C
158 700 -1.0 85 83 U=3 IMP:P=1 \$ OUTSIDE WELL
159 800 -0.001205 81 U=4 IMP:P=1 \$ OUTSIDE COOLER
160 800 -0.001205 -82 U=3 IMP:P=1 \$ INNER PU-238 WELL
161 100 -7.92 -83 82 U=3 IMP:P=1 \$ PU-238 WELL WALL
162 100 -7.92 -85 83 U=3 IMP:P=1 \$ ENDCAP
164 0 -84 U=4 FILL=3 TRCL=75 IMP:P=1 \$ WELL 1
165 0 -84 U=4 FILL=3 TRCL=76 IMP:P=1 \$ WELL 2
166 0 -84 U=4 FILL=3 TRCL=77 IMP:P=1 \$ WELL 3
167 0 -84 U=4 FILL=3 TRCL=78 IMP:P=1 \$ WELL 4
168 0 -84 U=4 FILL=3 TRCL=79 IMP:P=1 \$ WELL 5
169 0 -84 U=4 FILL=3 TRCL=80 IMP:P=1 \$ WELL 6
170 0 -84 U=4 FILL=3 TRCL=81 IMP:P=1 \$ WELL 7
171 0 -84 U=4 FILL=3 TRCL=82 IMP:P=1 \$ WELL 8
172 0 -84 U=4 FILL=3 TRCL=83 IMP:P=1 \$ WELL 9
173 0 -84 U=4 FILL=3 TRCL=84 IMP:P=1 \$ WELL 10
174 0 -84 U=4 FILL=3 TRCL=85 IMP:P=1 \$ WELL 11
175 0 -84 U=4 FILL=3 TRCL=86 IMP:P=1 \$ WELL 12
176 100 -7.92 -81 80 U=4 IMP:P=1 \$ COOLER WALL

177 700 -1.0 #164 #165 #166 #167
#168 #169 #170 #171
#172 #173 #174 #175
-80 U=4 IMP:P=1 \$ INSIDE COOLER
178 0 -78 FILL=4 TRCL=74 IMP:P=1 \$ CELL 1 COOLER
C
C CELL 2 COOLER
C
180 800 -0.001205 -88 U=5 IMP:P=1 \$ INNER PU-238 WELL
181 100 -7.92 -89 88 U=5 IMP:P=1 \$ PU-238 WELL WALL
182 100 -7.92 -91 89 U=5 IMP:P=1 \$ ENDCAP
184 0 -90 U=6 FILL=5 TRCL=88 IMP:P=1 \$ WELL 1
185 0 -90 U=6 FILL=5 TRCL=89 IMP:P=1 \$ WELL 2
186 0 -90 U=6 FILL=5 TRCL=90 IMP:P=1 \$ WELL 3
187 0 -90 U=6 FILL=5 TRCL=91 IMP:P=1 \$ WELL 4
188 100 -7.92 -87 86 U=6 IMP:P=1 \$ COOLER WALL
189 700 -1.0 #184 #185 #186 #187
-86 U=6 IMP:P=1 \$ INSIDE COOLER
190 0 -79 FILL=6 TRCL=87 IMP:P=1 \$ CELL 2 COOLER
191 700 -1.0 91 89 U=5 IMP:P=1 \$ OUTSIDE WELL
192 800 -0.001205 87 U=6 IMP:P=1 \$ OUTSIDE COOLER
C
C CELL 2 LARGE COOLER
C
200 800 -0.001205 -94 IMP:P=1 \$ INNER PU-238 WELL
201 100 -7.92 -95 94 IMP:P=1 \$ PU-238 WELL WALL
202 100 -7.92 -96 -97 95 IMP:P=1 \$ PU-238 WELL ENDCAP
203 700 -1.0 -96 97 95 IMP:P=1 \$ WATER SURROUNDING WELL
204 700 -1.0 -92 96 IMP:P=1 \$ INSIDE COOLER
205 100 -7.92 -93 92 IMP:P=1 \$ COOLER WALL
206 300 -11.34 -98 93 IMP:P=1 \$ LEAD JACKET
C
C TRANSFER TUBES
C
210 800 -0.001205 -68 -6 IMP:P=1 \$ INNER TUBE CELLS 1-2
211 800 -0.001205 -68 -16 IMP:P=1 \$ INNER TUBE CELLS 2-3
212 800 -0.001205 -68 -26 IMP:P=1 \$ INNER TUBE CELLS 3-4
213 800 -0.001205 -68 -36 IMP:P=1 \$ INNER TUBE CELLS 4-5
214 100 -7.92 -69 68 -6 IMP:P=1 \$ INNER TUBE CELLS 1-2
215 100 -7.92 -69 68 -16 IMP:P=1 \$ INNER TUBE CELLS 2-3
216 100 -7.92 -69 68 -26 IMP:P=1 \$ INNER TUBE CELLS 3-4
217 100 -7.92 -69 68 -36 IMP:P=1 \$ INNER TUBE CELLS 4-5
C
C VOID CELLS
C
996 800 -0.001205 -101 -75 IMP:P=1 \$ VOID BENEATH COLLIMATORS
997 800 -0.001205 #83 #84 #85 #86 #87
#88 #89 #90 #91 #92
#93 #94 #95 #96 #97
#98 #99 #100 #101 #102
#103 #104 #105 #106 #107
#108 #109 #110 #111 #112
#113 #114 #115 #116 #117

```
#118 #119 #120 #121 #122
#123 #124 #125 #126 #127
#128 #129 #130 #131 #132
#133 #134 #135 #136 #137
#138 #139 #140 #141 #142
#143 #144 #145 #146 #147
#148 #149 #150 #151 #152
-101 -74 75 IMP:P=1 $ VOID SURROUNDING COLLIMATORS
998 800 -0.001205 -101 100 24 34 44
#76 #77 #78 74 #178
#190 98 IMP:P=1 $ VOID SURROUNDING CELLS
999 0 101 IMP:P=0 $ THE GRAVEYARD

C CCCCCCCCCCCCCCCCCCCCCCCCCCCCCCCCCCCCCCCCCCCCCCCCCCCCCCCCCCCCCCCC
C
C SURFACE CARDS
C
C CCCCCCCCCCCCCCCCCCCCCCCCCCCCCCCCCCCCCCCCCCCCCCCCCCCCCCCCCCCCCCCC
C
C CELL 1
C
1 RPP 0. 512.45 0. 152.4 0. 208.28 $ INTERIOR
2 RPP -0.32 512.76 -0.32 152.72 -0.476 208.6 $ EXTERIOR
3 RPP -0.32 512.76 -0.32 152.72 -8.096 -0.476 $ GIRDERS
4 RPP 36.83 90.17 90.17 143.51 -8.096 -0.476 $ FURNACE 1 CUTOUT
5 RPP 322.26 375.60 90.17 143.51 -8.096 -0.476 $ FURNACE 2 CUTOUT
6 RPP 512.76 523.88 -0.32 152.72 -8.096 208.6 $ CELL GAP
7 PZ 30 $ MATERIAL FILL
8 RPP 266.84 297.03 131.45 147.00 89.52 119.71 $ INNER HEPA
9 RPP 266.54 297.34 131.45 147.00 89.22 120.02 $ HEPA BOX
C
C CELL 2
C
11 RPP 524.19 726.12 0. 152.4 0. 208.28 $ INTERIOR
12 RPP 523.88 726.44 -0.32 152.72 -0.476 208.6 $ EXTERIOR
13 RPP 523.88 726.44 -0.32 152.72 -8.096 -0.476 $ GIRDERS
16 RPP 726.44 737.55 -0.32 152.72 -8.096 208.6 $ CELL GAP
17 PZ 30 $ MATERIAL FILL
18 RPP 641.81 672.00 131.45 147.00 89.52 119.71 $ INNER HEPA
19 RPP 641.51 672.31 131.45 147.00 89.22 120.02 $ HEPA BOX
C
C CELL 3
C
21 RPP 737.87 939.80 0. 152.4 0. 208.28 $ INTERIOR
22 RPP 737.55 940.12 -0.32 152.72 -0.476 208.6 $ EXTERIOR
23 RPP 737.55 940.12 -0.32 152.72 -8.096 -0.476 $ GIRDERS
24 RCC 785.50 52.07 -8.096 0. 0. -50.96 24.13 $ COOLER EXT
25 RCC 785.50 52.07 -8.096 0. 0. -49.45 22.62 $ COOLER INT
26 RPP 940.12 951.23 -0.32 152.72 -8.096 208.6 $ CELL GAP
27 PZ 30 $ MATERIAL FILL
28 RPP 790.72 820.91 131.45 147.00 89.52 119.71 $ INNER HEPA
29 RPP 790.42 821.21 131.45 147.00 89.22 120.02 $ HEPA BOX
C
```

C CELL 4

C

31 RPP 951.55 1215.39 0. 152.4 0. 208.28 \$ INTERIOR
32 RPP 951.23 1215.71 -0.32 152.72 -0.476 208.6 \$ EXTERIOR
33 RPP 951.23 1215.71 -0.32 152.72 -8.096 -0.476 \$ GIRDERS
34 RCC 1170.15 52.07 -8.096 0. 0. -50.96 27.94 \$ COOLER EXT
35 RCC 1170.15 52.07 -8.096 0. 0. -49.45 26.43 \$ COOLER INT
36 RPP 1215.71 1226.82 -0.32 152.72 -8.096 208.6 \$ CELL GAP
37 PZ 30 \$ MATERIAL FILL
38 RPP 1073.45 1103.64 131.45 147.00 89.52 119.71 \$ INNER HEPA
39 RPP 1073.15 1103.95 131.45 147.00 89.22 120.02 \$ HEPA BOX

C

C CELL 5

C

41 RPP 1227.14 1501.46 0. 152.4 0. 208.28 \$ INTERIOR
42 RPP 1226.82 1501.78 -0.32 152.72 -0.476 208.6 \$ EXTERIOR
43 RPP 1226.82 1501.78 -0.32 152.72 -8.096 -0.476 \$ GIRDERS
44 RCC 1402.40 52.07 -8.096 0. 0. -50.96 27.94 \$ COOLER EXT
45 RCC 1402.40 52.07 -8.096 0. 0. -49.45 26.43 \$ COOLER INT
46 RPP 1264.29 1317.63 90.17 143.51 -8.096 -0.476 \$ FURNACE CUTOUT
47 PZ 30 \$ MATERIAL FILL
48 RPP 1308.56 1338.75 131.45 147.00 89.52 119.71 \$ INNER HEPA
49 RPP 1308.26 1339.06 131.45 147.00 89.22 120.02 \$ HEPA BOX

C

C FURNACE

C

51 RCC 0 0 -79.02 0 0 79.02 17.28 \$ SKIN OUTER SURFACE
52 RCC 0 0 -78.38 0 0 78.38 17.16 \$ SKIN INNER SURFACE
53 RCC 0 0 -78.07 0 0 78.07 15.88 \$ INNER SHELL OUTER SURFACE
54 RCC 0 0 -77.27 0 0 77.27 15.57 \$ INNER SHELL INNER SURFACE
55 RCC 0 0 -64.57 0 0 44.70 7.77 \$ HEATING ELEMENT OUTER
56 RCC 0 0 -67.11 0 0 67.11 7.62 \$ HEATER TUBE OUTER
57 RCC 0 0 -65.84 0 0 65.84 6.99 \$ HEATER TUBE INNER
58 RCC 0 0 -64.57 0 0 64.57 6.67 \$ WORK TUBE OUTER
59 RCC 0 0 -63.94 0 0 63.94 6.03 \$ WORK TUBE INNER
60 RCC 0 0 -35.11 0 0 35.11 1.91 \$ SAMPLE SUPPORT TUBE OUTER
61 RCC 0 0 -35.11 0 0 35.11 1.60 \$ SAMPLE SUPPORT TUBE INNER
62 RCC 0 0 -63.94 0 0 28.83 5.72 \$ SAMPLE HOLDER
63 PZ -31.30 \$ WORK TUBE LOWER INSUL.
64 PZ -24.95 \$ WORK TUBE UPPER INSUL.
65 RCC 0 0 -78.38 0 0 78.38 16.85 \$ MIDDLE SHELL OUTER SURFACE
66 RCC 0 0 -78.38 0 0 78.38 16.29 \$ MIDDLE SHELL INNER SURFACE
67 RCC 0 0 -79.021 0 0 79.022 17.281 \$ FURNACE FILL SURFACE

C

C TRANSFER TUBE

C

68 C/X 116.84 27.94 19.84 \$ INNER TRANSFER TUBE
69 C/X 116.84 27.94 20.32 \$ OUTER TRANSFER TUBE

C

C COLLIMATOR

C

70 RCC 0 0 0 0 -10.16 2.06 \$ INNER WALL CENTRAL TUBE
71 RCC 0 0 0 0 -10.16 2.22 \$ OUTER WALL CENTRAL TUBE

[illegible]

```
C
C TURN OFF BREMSSTRAHLUNG PRODUCTION
C
PHYS:P 100 1 0 0 0
C
C KILL PHOTONS BENEATH 95 keV
C
CUT:P j 0.095
C
C CCCCCCCCCCCCCCCCCCCCCCCCCCCCCCCCCCCCCCCCCCCCCCCCCCCCCCCCCCCCCCCCCCCCCCCC
C
C TRANSLATION CARDS
C
C CCCCCCCCCCCCCCCCCCCCCCCCCCCCCCCCCCCCCCCCCCCCCCCCCCCCCCCCCCCCCCCCCCCCCCCC
C
TR1   63.5    116.84   -0.482   $ FURNACE 1 CELL 1
TR2   348.93   116.84   -0.482   $ FURNACE 2 CELL 1
TR3   1290.96  116.84   -0.482   $ FURNACE  CELL 5
TR4    23.77   49.53   -94.46   $ CELL 1 COLLIMATOR 2
TR5    19.91           74.30     -94.46   $ CELL 1 COLLIMATOR 3
TR6    19.91          106.68   -94.46   $ CELL 1 COLLIMATOR 4
TR7    77.79           40.96     -94.46   $ CELL 1 COLLIMATOR 5
TR8    72.28           66.68     -94.46   $ CELL 1 COLLIMATOR 6
TR9    105.35          40.96     -94.46   $ CELL 1 COLLIMATOR 8
TR10   105.35          77.79     -94.46   $ CELL 1 COLLIMATOR 9
TR11   105.35          111.44   -94.46   $ CELL 1 COLLIMATOR 10
TR12   149.45          111.44   -94.46   $ CELL 1 COLLIMATOR 11
TR13   164.15          77.79     -94.46   $ CELL 1 COLLIMATOR 12
TR14   183.75          44.45     -94.46   $ CELL 1 COLLIMATOR 13
TR15   193.55          77.79     -94.46   $ CELL 1 COLLIMATOR 14
TR16   193.55          111.44   -94.46   $ CELL 1 COLLIMATOR 15
TR17   235.20          111.44   -94.46   $ CELL 1 COLLIMATOR 16
TR18   237.65          77.79     -94.46   $ CELL 1 COLLIMATOR 17
TR19   235.20          43.82     -94.46   $ CELL 1 COLLIMATOR 18
TR20   298.29          43.82     -94.46   $ CELL 1 COLLIMATOR 19
TR21   298.29          77.79     -94.46   $ CELL 1 COLLIMATOR 20
TR22   298.29          111.44   -94.46   $ CELL 1 COLLIMATOR 21
TR23   333.81          77.79     -94.46   $ CELL 1 COLLIMATOR 22
TR24   333.81          40.96     -94.46   $ CELL 1 COLLIMATOR 23
TR25   369.95          40.96     -94.46   $ CELL 1 COLLIMATOR 24
TR26   369.95          77.79     -94.46   $ CELL 1 COLLIMATOR 25
TR27   367.01          111.44   -94.46   $ CELL 1 COLLIMATOR 26
TR28   426.30          111.44   -94.46   $ CELL 1 COLLIMATOR 27
TR29   432.12          77.79     -94.46   $ CELL 1 COLLIMATOR 28
TR30   457.54          111.44   -94.46   $ CELL 1 COLLIMATOR 29
TR31   474.69          88.27     -94.46   $ CELL 1 COLLIMATOR 30
TR32   479.59          40.96     -94.46   $ CELL 1 COLLIMATOR 31
TR33   518.32   116.52   -94.46   $ CELL 2 COLLIMATOR 32
TR34   558.48          111.44   -94.46   $ CELL 2 COLLIMATOR 33
TR35   558.48          75.25     -94.46   $ CELL 2 COLLIMATOR 34
```

TR36	595.95	40.96	-94.46	\$ CELL 2 COLLIMATOR 35
TR37	625.79	118.11	-94.46	\$ CELL 2 COLLIMATOR 36
TR38	657.54	116.52	-94.46	\$ CELL 2 COLLIMATOR 37
TR39	668.34	81.28	-94.46	\$ CELL 2 COLLIMATOR 38
TR40	695.65	43.82	-94.46	\$ CELL 2 COLLIMATOR 39
TR41	695.65	76.20	-94.46	\$ CELL 2 COLLIMATOR 40
TR42	710.88	111.44	-94.46	\$ CELL 2 COLLIMATOR 41
TR43	759.14	78.74	-94.46	\$ CELL 3 COLLIMATOR 1
TR44	742.95	40.96	-94.46	\$ CELL 3 COLLIMATOR 2
TR45	795.66	80.01	-94.46	\$ CELL 3 COLLIMATOR 3
TR46	795.66	111.44	-94.46	\$ CELL 3 COLLIMATOR 4
TR47	854.08	111.44	-94.46	\$ CELL 3 COLLIMATOR 5
TR48	854.08	77.15	-94.46	\$ CELL 3 COLLIMATOR 6
TR49	852.49	40.96	-94.46	\$ CELL 3 COLLIMATOR 7
TR50	905.51	40.96	-94.46	\$ CELL 3 COLLIMATOR 8
TR51	905.51	76.20	-94.46	\$ CELL 3 COLLIMATOR 9
TR52	905.51	111.44	-94.46	\$ CELL 3 COLLIMATOR 10
TR53	974.41	111.44	-94.46	\$ CELL 4 COLLIMATOR 11
TR54	971.55	76.20	-94.46	\$ CELL 4 COLLIMATOR 12
TR55	977.27	40.96	-94.46	\$ CELL 4 COLLIMATOR 13
TR56	1034.42	40.96	-94.46	\$ CELL 4 COLLIMATOR 14
TR57	1034.42	80.01	-94.46	\$ CELL 4 COLLIMATOR 15
TR58	1034.42	111.44	-94.46	\$ CELL 4 COLLIMATOR 16
TR59	1083.95	111.44	-94.46	\$ CELL 4 COLLIMATOR 17
TR60	1083.95	76.20	-94.46	\$ CELL 4 COLLIMATOR 18
TR61	1084.26	40.96	-94.46	\$ CELL 4 COLLIMATOR 19
TR62	1131.25	40.96	-94.46	\$ CELL 4 COLLIMATOR 20
TR63	1141.10	88.58	-94.46	\$ CELL 4 COLLIMATOR 21
TR64	1158.24	111.44	-94.46	\$ CELL 4 COLLIMATOR 22
TR65	1210.31	116.84	-94.46	\$ CELL 4 COLLIMATOR 23
TR66	1241.43	40.96	-94.46	\$ CELL 5 COLLIMATOR 24
TR67	1229.68	72.39	-94.46	\$ CELL 5 COLLIMATOR 25
TR68	1260.79	111.44	-94.46	\$ CELL 5 COLLIMATOR 26
TR69	1261.43	71.44	-94.46	\$ CELL 5 COLLIMATOR 27
TR70	1304.29	76.20	-94.46	\$ CELL 5 COLLIMATOR 28
TR71	1330.01	40.96	-94.46	\$ CELL 5 COLLIMATOR 29
TR72	1389.70	105.73	-94.46	\$ CELL 5 COLLIMATOR 30
TR73	1402.40	77.72	-94.46	\$ CELL 5 COLLIMATOR 31
TR74	447.99	52.07	-0.482	\$ CELL 1 COOLER
TR75	0.0	8.53	-1.432	\$ WELL 1 CELL 1 COOLER
TR76	8.53	0.0	-1.432	\$ WELL 2 CELL 1 COOLER
TR77	-8.53	0.0	-1.432	\$ WELL 3 CELL 1 COOLER
TR78	0.0	-8.53	-1.432	\$ WELL 4 CELL 1 COOLER
TR79	-8.53	17.06	-1.432	\$ WELL 5 CELL 1 COOLER
TR80	8.53	17.06	-1.432	\$ WELL 6 CELL 1 COOLER
TR81	17.06	-8.53	-1.432	\$ WELL 7 CELL 1 COOLER
TR82	17.06	8.53	-1.432	\$ WELL 8 CELL 1 COOLER
TR83	8.53	-17.06	-1.432	\$ WELL 9 CELL 1 COOLER
TR84	-8.53	-17.06	-1.432	\$ WELL 10 CELL 1 COOLER
TR85	-17.06	8.53	-1.432	\$ WELL 11 CELL 1 COOLER
TR86	-17.06	-8.53	-1.432	\$ WELL 12 CELL 1 COOLER
TR87	561.66	52.07	-0.482	\$ CELL 2 COOLER
TR88	7.62	7.62	-1.432	\$ WELL 1 CELL 2 COOLER

				\$ WELL 2	CELL 2 COOLER
TR89	-7.62	-7.62	-1.432	\$ WELL 3	CELL 2 COOLER
TR90	-7.62	-7.62	-1.432	\$ WELL 4	CELL 2 COOLER
C					
C	CC				
C					
C	MATERIAL CARDS				
C					
C	CC				
C					
C	STAINLESS STEEL 316, DENSITY = 7.92 g/cm^3				
C					
M100	14000	-0.010		\$ Si	
	24000	-0.170		\$ Cr	
	25000	-0.020		\$ Mn	
	26000	-0.655		\$ Fe	
	28000	-0.120		\$ Ni	
	42000	-0.025		\$ Mo	
C					
C	CARBON STEEL, DENSITY = 7.82 g/cc				
C					
M200	6000	-0.005		\$ C	
	26000	-0.995		\$ Fe	
C					
C	LEAD, DENSITY = 11.34 g/cm^3				
C					
M300	82000	1.0		\$ Pb	
C					
C	BOROSILICATE FIBERGLASS FILTER, DENSITY = 0.02 g/cm^3				
C					
M400	5000	-0.040063		\$ B	
	8000	-0.539561		\$ O	
	11000	-0.028191		\$ Na	
	13000	-0.011644		\$ Al	
	14000	-0.377220		\$ Si	
	19000	-0.003321		\$ K	
C					
C					
C	ALUMINUM OXIDE, DENSITY = 3.75-3.95 g/cm^3				
C					
M500	8000	0.6		\$ O	
	13000	0.4		\$ Al	
C					
C	TUNGSTEN, DENSITY = 19.3 g/cm^3				
C					
M600	74000	1.0		\$ W	
C					
C	WATER, DENISTY = 1.0 g/cm^3				
C					
M700	1000	0.666667		\$ H	
	8000	0.333333		\$ O	
C					
C	AIR, DENSITY = 0.001205 g/cm^3				

```
C
M800    6000   0.000124 $ C
      7000   0.755268 $ N
          8000   0.231781 $ O
         18000   0.012827 $ Ar
C
C TUNGSTEN SHOT : BULK DENSITY = 9.6 g/cc
C
M900 26000 -0.1    $ Fe
     28000 -0.2    $ Ni
     74000 -0.7    $ W
C
CCCCCCCCCCCCCCCCCCCCCCCCCCCCCCCCCCCCCCCCCCCCCCCCCCCCCCCCCCCCCCCCCC
C
C SOURCE CARDS
C
CCCCCCCCCCCCCCCCCCCCCCCCCCCCCCCCCCCCCCCCCCCCCCCCCCCCCCCCCCCCCCCCCC
C
C
SDEF PAR=P           $ PHOTON SOURCE
  ERG=D1             $ ENERGY GIVEN BY DISTRIBUTION 1
  X=D2               $ SOURCE DISTRIBUTION IN X
  Y=D3              $ SOURCE DISTIRBUTION IN Y
  Z=D4              $ SOURCE DISTIRBUTION IN Z
  CEL = CELL_NUM    $ VARIABLE CELL NUMBER
  VEC = 0 0 -1      $ REFERENCE DIRECTION IS -Z
  DIR = D5          $ INITIAL DIRECTION DISTRIBUTION
C
C ENERGY DISTRIBUTION (DISCRETE LINES)
C
SI1 L 0.099853
    0.152720
    0.76639
C
C ENERGY DISTRIBUTION PROBABILITIES (UNNORMALIZED)
C
SP1 1.
    1.
    1.
C
C SOURCE DISTRIBUTION IN X - UNIFORM OVER EXTENT OF CELLS
C
SI2 H -0.1 1502.
SP2 0. 1.
C
C SOURCE DISTRIBUTION IN Y - UNIFORM OVER EXTENT OF CELLS
C
SI3 H -0.1 153.
SP3 0. 1.
C
C SOURCE DISTRIBUTION IN Z - UNIFORM OVER EXTENT OF CELLS
C
SI4 H -0.1 30.1
```

```
SP4 0. 1.  
C  
C SOURCE INITIAL MOMENTUM DISTRIBUTION  
C ONLY EMIT PHOTONS DIRECTED DOWNWARDS  
C NO EMISSION FROM COS(THETA)=-1 TO 0.9  
C EQUIPROBABLE EMISSION BETWEEN COS(THETA)= 0.9 TO 1  
C  
SI5 H 0.9 1.  
SP5 0. 1.  
C  
C CCCCCCCCCCCCCCCCCCCCCCCCCCCCCCCCCCCCCCCCCCCCCCCCCCCCCCCCCCCCCCCCCCCCCCCC  
C  
C TALLY CARDS  
C  
C CCCCCCCCCCCCCCCCCCCCCCCCCCCCCCCCCCCCCCCCCCCCCCCCCCCCCCCCCCCCCCCCCCCCCCCC  
C  
E5 0. 0.099 0.1 0.152 0.153 0.766 0.767 $ TALLY 5 ENERGY BINS  
C  
FC5 PHOTON FLUX AT CELL 1 ASSAY POSITIONS  
C  
F5:P 23.77 49.53 -104.62 0  
    19.91 74.30 -104.62 0  
    19.91 106.68 -104.62 0  
    77.79 40.96 -104.62 0  
    72.28 66.68 -104.62 0  
    105.35 40.96 -104.62 0  
    105.35 77.79 -104.62 0  
    105.35 111.44 -104.62 0  
    149.45 111.44 -104.62 0  
    164.15 77.79 -104.62 0  
    183.75 44.45 -104.62 0  
    193.55 77.79 -104.62 0  
    193.55 111.44 -104.62 0  
    235.20 111.44 -104.62 0  
    237.65 77.79 -104.62 0  
    235.20 43.82 -104.62 0  
    298.29 43.82 -104.62 0  
    298.29 77.79 -104.62 0  
    298.29 111.44 -104.62 0  
    333.81 77.79 -104.62 0  
    333.81 40.96 -104.62 0  
    369.95 40.96 -104.62 0  
    369.95 77.79 -104.62 0  
    367.01 111.44 -104.62 0  
    426.30 111.44 -104.62 0  
    432.12 77.79 -104.62 0  
    457.54 111.44 -104.62 0  
    474.69 88.27 -104.62 0  
    479.59 40.96 -104.62 0  
C  
E15 0. 0.099 0.1 0.152 0.153 0.766 0.767 $ TALLY 15 ENERGY BINS  
C  
FC15 PHOTON FLUX AT CELL 2 ASSAY POSITIONS
```

C

F15:P 518.32 116.52 -104.62 0

558.48 111.44 -104.62 0

558.48 75.25 -104.62 0

595.95 40.96 -104.62 0

625.79 118.11 -104.62 0

657.54 116.52 -104.62 0

668.34 81.28 -104.62 0

695.65 43.82 -104.62 0

695.65 76.20 -104.62 0

710.88 111.44 -104.62 0

C

E25 0. 0.099 0.1 0.152 0.153 0.766 0.767 \$ TALLY 25 ENERGY BINS

C

FC25 PHOTON FLUX AT CELL 3 ASSAY POSITIONS

C

F25:P 759.14 78.74 -104.62 0

742.95 40.96 -104.62 0

795.66 80.01 -104.62 0

795.66 111.44 -104.62 0

854.08 111.44 -104.62 0

854.08 77.15 -104.62 0

852.49 40.96 -104.62 0

905.51 40.96 -104.62 0

905.51 76.20 -104.62 0

905.51 111.44 -104.62 0

C

E35 0. 0.099 0.1 0.152 0.153 0.766 0.767 \$ TALLY 35 ENERGY BINS

C

FC35 PHOTON FLUX AT CELL 4 ASSAY POSITIONS

C

F35:P 974.41 111.44 -104.62 0

971.55 76.20 -104.62 0

977.27 40.96 -104.62 0

1034.42 40.96 -104.62 0

1034.42 80.01 -104.62 0

1034.42 111.44 -104.62 0

1083.95 111.44 -104.62 0

1083.95 76.20 -104.62 0

1084.26 40.96 -104.62 0

1131.25 40.96 -104.62 0

1141.10 88.58 -104.62 0

1158.24 111.44 -104.62 0

1210.31 116.84 -104.62 0

C

E45 0. 0.099 0.1 0.152 0.153 0.766 0.767 \$ TALLY 45 ENERGY BINS

C

FC45 PHOTON FLUX AT CELL 5 ASSAY POSITIONS

C

F45:P 1241.43 40.96 -104.62 0

1229.68 72.39 -104.62 0

1260.79 111.44 -104.62 0

1261.43 71.44 -104.62 0

1304.29 76.20 -104.62 0
1330.01 40.96 -104.62 0
1389.70 105.73 -104.62 0
1402.40 77.72 -104.62 0

C

FC4 PHOTON FLUX AT CELL 1 ASSAY POSITIONS (THIN DISK DETECTOR)

C

F4:P (154<83)

(154<84)
(154<85)
(154<86)
(154<87)
(154<88)
(154<89)
(154<90)
(154<91)
(154<92)
(154<93)
(154<94)
(154<95)
(154<96)
(154<97)
(154<98)
(154<99)
(154<100)
(154<101)
(154<102)
(154<103)
(154<104)
(154<105)
(154<106)
(154<107)
(154<108)
(154<109)
(154<110)
(154<111)

C

E4 0. 1998i 1.0 \$ DISK DETECTOR TALLY ENERGY BINS

C

C SPLITS TALLY 4 INTO THREE TALLIES ONE FOR EACH SOURCE ENERGY

C

FT4 SCX 1

C

FC14 PHOTON FLUX AT CELL 2 ASSAY POSITIONS (THIN DISK DETECTOR)

C

F14:P (154<112)

(154<113)
(154<114)
(154<115)
(154<116)
(154<117)
(154<118)
(154<119)

(154<120)
(154<121)
C
E14 0. 1998i 1.0 \$ DISK DETECTOR TALLY ENERGY BINS
C
C SPLITS TALLY 14 INTO THREE TALLIES ONE FOR EACH SOURCE ENERGY
C
FT14 SCX 1
C
FC24 PHOTON FLUX AT CELL 3 ASSAY POSITIONS (THIN DISK DETECTOR)
C
F24:P (154<122)
 (154<123)
 (154<124)
 (154<125)
 (154<126)
 (154<127)
 (154<128)
 (154<129)
 (154<130)
 (154<131)
C
E24 0. 1998i 1.0 \$ DISK DETECTOR TALLY ENERGY BINS
C
C SPLITS TALLY 24 INTO THREE TALLIES ONE FOR EACH SOURCE ENERGY
C
FT24 SCX 1
C
FC34 PHOTON FLUX AT CELL 4 ASSAY POSITIONS (THIN DISK DETECTOR)
C
F34:P (154<132)
 (154<133)
 (154<134)
 (154<135)
 (154<136)
 (154<137)
 (154<138)
 (154<139)
 (154<140)
 (154<141)
 (154<142)
 (154<143)
 (154<144)
C
E34 0. 1998i 1.0 \$ DISK DETECTOR TALLY ENERGY BINS
C
C SPLITS TALLY 34 INTO THREE TALLIES ONE FOR EACH SOURCE ENERGY
C
FT34 SCX 1
C
FC44 PHOTON FLUX AT CELL 4 ASSAY POSITIONS (THIN DISK DETECTOR)
C
F44:P (154<145)

C
C
C ASSAY SIMULATION FOR PuFF OXYGEN EXCHANGE FURNACE
C
C
C CC
C
C SIMULATION OF PuFF OXYGEN EXCHANGE FURNACE WITH Pu-238 GAMMA
C SOURCES (99, 153, AND 766 keV LINES ONLY). VARIED SOURCE
C DISTRIBUTIONS AND QUANTITIES OF ATTENUATING MATERIALS WILL
C BE SIMULATED TO ESTIMATE UNCERTAINTY.
C
C THERE IS A GAP BETWEEN THE INNER AND OUTER SHELLS THROUGH
C WHICH COOLING WATER WAS ONCE RUN. FOR THIS SIMULATION IT
C WILL BE ASSUMED THAT IT IS STILL FILLED WITH WATER
C
C BETWEEN THE INNER SHELL AND THE HEATER TUBE THERE IS A LAYER OF
C ALUMINA BUBBLE INSULATION. THIS IS MADE IN A VARIETY OF SIZES.
C IT IS UNKNOWN WHAT SIZE WAS USED. THE SIZES ADVERTIZED ON THE
C INTERNET VARY BETWEEN 30 AND 65 lbs/ft^3. THE MID-RANGE DENSITY
C WILL BE USED HERE, 0.76 g/cm^3.
C
C THE HEATING ELEMENT IS FOUR 1/16-INCH DIAMETER TUNGSTEN WIRES EACH
C 57 FEET LONG. THE TOTAL MASS OF TUNGSTEN IN THESE WIRES SHOULD BE
C 2655 GRAMS. THE VOLUME OF THE HEATING ELEMENT REGION IS 329.5 cm^3.
C THUS THE DENSITY IS 8.06 g/cm^3.
C
C THERE ARE NO DRAWINGS OF THE SAMPLE HOLDER. IT WILL BE ASSUMED TO
C WEIGH 1 kg AND BE COMPOSED OF ALUMINUM OXIDE. THIS GIVES A BULK
C DENSITY OF 0.32 g/cm^3.
C
C A TUNGSTEN SHOT COLLIMATOR WAS USED DURING THE ASSAYS WITH A BULK
C DENSITY OF 9.6 g/cm^3. THE STANDOFF DISTANCE WAS 46.5 INCHES FOR THE
C SOUTHERN FURNACE IN CELL 1 AND 68 INCHES FOR THE NORTHERN FURNACE.
C
C PHOTON ARE ONLY EMITTED WITH AN INITIAL MOMENTUM VECTOR WITH AN
C ANGLE RELATIVE TO THE +X AXIS SUCH THAT COS(THETA)> 0.9
C THIS IS IN THE GENERAL DIRECTION OF THE DETECTOR
C

[illegible]

C FURNACE

C

1	RCC	0 0	-79.02	0 0	79.02	17.28	\$ SKIN OUTER SURFACE
2	RCC	0 0	-78.38	0 0	78.38	17.16	\$ SKIN INNER SURFACE
3	RCC	0 0	-78.07	0 0	78.07	15.88	\$ INNER SHELL OUTER SURFACE
4	RCC	0 0	-77.27	0 0	77.27	15.57	\$ INNER SHELL INNER SURFACE
5	RCC	0 0	-64.57	0 0	36.14	7.77	\$ HEATING ELEMENT OUTER
6	RCC	0 0	-67.11	0 0	67.11	7.62	\$ HEATER TUBE OUTER
7	RCC	0 0	-65.84	0 0	65.84	6.99	\$ HEATER TUBE INNER
8	RCC	0 0	-64.57	0 0	64.57	6.67	\$ WORK TUBE OUTER
9	RCC	0 0	-63.94	0 0	63.94	6.03	\$ WORK TUBE INNER
10	RCC	0 0	-33.60	0 0	33.60	1.91	\$ SAMPLE SUPPORT TUBE OUTER
11	RCC	0 0	-33.60	0 0	33.60	1.60	\$ SAMPLE SUPPORT TUBE INNER
12	RCC	0 0	-63.94	0 0	30.33	5.72	\$ SAMPLE HOLDER
13	PZ		-29.79				\$ WORK TUBE LOWER INSUL.
14	PZ		-23.44				\$ WORK TUBE UPPER INSUL.
15	RCC	0 0	-78.38	0 0	78.38	16.85	\$ MIDDLE SHELL OUTER SURFACE
16	RCC	0 0	-78.38	0 0	78.38	16.29	\$ MIDDLE SHELL INNER SURFACE

C

C SURROUNDINGS

C

20 RPP	17.78	508.0	-100	100	-152.40	-91.44	\$ CONCRETE FLOOR
21 RPP	24.77	40.01	-100	100	-91.44	-87.63	\$ LOWER THRESHOLD 1
22 RPP	24.77	34.29	-100	100	-87.63	-77.31	\$ LOWER THRESHOLD 2
23 RPP	24.77	34.29	-100	100	-20.16	-0.48	\$ UPPER THRESHOLD 1
24 RPP	34.29	54.29	-100	100	-6.03	-0.48	\$ UPPER THRESHOLD 2
25 RPP	40.01	54.29	-100	100	-0.48	11.11	\$ UPPER THRESHOLD 3
26 RPP	34.29	54.29	-100	100	-6.99	-6.03	\$ LEAD LINER 1
27 RPP	54.29	55.25	-100	100	-6.99	11.11	\$ LEAD LINER 2

C

C COLLIMATOR

C

30	RCC	135.39	0	-45.72	10.16	0	0	2.06	\$ INNER WALL CENTRAL TUBE
31	RCC	135.39	0	-45.72	10.16	0	0	2.22	\$ OUTER WALL CENTRAL TUBE
32	RCC	135.39	0	-45.72	15.88	0	0	8.41	\$ OUTER COLLIMATOR WALL
33	RCC	145.55	0	-45.72	5.72	0	0	3.81	\$ DETECTOR VOID WALL
34	RCC	145.55	0	-45.72	0.01	0	0	2.06	\$ DETECTION REGION

C

99 RPP -100 1000 -200 200 -250 100 \$ GRAVEYARD FENCE

[illegible]

C

C DATA CARDS

C

[illegible]

C

MODE P	\$ TRANSPORT PHOTONS
NPS 5e9	\$ 5 BILLION SOURCE PHOTONS
PRINT 10	\$ PRINT SOURCE COEFFICIENTS AND DISTRIBUTION
40	\$ PRINT MATERIAL COMPOSITION
50	\$ PRINT CELL VOLUME AND MASSES
110	\$ PRINT FIRST 50 STARTING HISTORIES
140	\$ PRINT NEUTRON/PHOTON NUCLIDE ACTIVITY

52

```
C
M400    82000   1.0      $ Pb
C
C ALUMINUM OXIDE, DENSITY = 3.75-3.95 g/cm^3
C
M500     8000   0.6       $ O
        13000   0.4       $ Al
C
C TUNGSTEN, DENSITY = 19.3 g/cm^3
C
M600     74000   1.0       $ W
C
C WATER, DENISTY = 1.0 g/cm^3
C
M700     1000   0.666667   $ H
        8000    0.333333   $ O
C
C AIR, DENSITY = 0.001205 g/cm^3
C
M800     6000   0.000124   $ C
        7000    0.755268   $ N
           8000   0.231781   $ O
          18000   0.012827   $ Ar
C
C TUNGSTEN SHOT : BULK DENSITY = 9.6 g/cc
C
M900    26000 -0.1       $ Fe
         28000 -0.2       $ Ni
         74000 -0.7       $ W
C
C CCCCCCCCCCCCCCCCCCCCCCCCCCCCCCCCCCCCCCCCCCCCCCCCCCCCCCCCCCCCCCCC
C
C SOURCE CARDS
C
C CCCCCCCCCCCCCCCCCCCCCCCCCCCCCCCCCCCCCCCCCCCCCCCCCCCCCCCCCCCCCCC
C
C
SDEF PAR=P             $ PHOTON SOURCE
ERG=D1                 $ ENERGY GIVEN BY DISTRIBUTION 1
POS= 0 0 -63.95       $ SOURCE DISTRIBUTION REFERENCE POSITION
RAD=D2                  $ RADIAL DISTRIBUTION (DISK)
EXT=D3                   $ VERTICAL BOUNDS
AXS= 0 0 1              $ PERPENDICULAR TO Z-AXIS
CEL=18                   $ SOURCE IN SAMPLE HOLDER
VEC = 1 0 0            $ REFERENCE DIRECTION IS +X
DIR = D5                 $ INITIAL DIRECTION DISTRIBUTION
C
C ENERGY DISTRIBUTION (DISCRETE LINES)
C
SI1 L 0.099853
    0.152720
    0.76639
C
```

```
C ENERGY DISTRIBUTION PROBABILITIES (UNNORMALIZED)
C
SP1 1.
    1.
    1.
C
C UNIFORM 2D RADIAL DISTRIBUTION
C
SI2 H 0. 5.73 $ 5.74 cm RADIUS
C
SP2 -21 1 $ PROPORTIONAL TO R
C
C UNIFORM VERTICAL DISTRIBUTION
C
SI3 H 0. 30.31 $ HEIGHT OF DISTRIBUTION
C
SP3 -21 0 $ UNIFORM IN Z
C
C SOURCE INITIAL MOMENTUM DISTRIBUTION
C ONLY EMIT PHOTONS DIRECTED TOWARDS DETECTOR
C NO EMISSION FROM COS(THETA)= -1 TO 0.9
C EQUIPROBABLE EMISSION BETWEEN COS(THETA) = 0.9 TO 1
C
SI5 H 0.9 1.
SP5 0. 1.
C
CCCCCCCCCCCCCCCCCCCCCCCCCCCCCCCCCCCCCCCCCCCCCCCCCCCCCCCCCCCCCC
C
C TALLY CARDS
C
CCCCCCCCCCCCCCCCCCCCCCCCCCCCCCCCCCCCCCCCCCCCCCCCCCCCCCCCCCCCCC
C
F5:P 145.55      0.00      -45.72 0.
C
FC5 PHOTON FLUX AT ASSAY POSITION (POINT DETECTOR)
C
E5 0. 0.099 0.1 0.152 0.153 0.766 0.767 $ POINT DETECTOR TALLY ENERGY BINS
C
F4:P 43
C
FC4 PHOTON FLUX AT ASSAY POSITION (THIN DISK DETECTOR)
C
E4 0. 1.998i 1.0          $ DISK DETECTOR TALLY ENERGY BINS
C
C SPLITS TALLY 4 INTO THREE TALLIES ONE FOR EACH SOURCE ENERGY
C
FT4 SCX 1
```

Example for Cell 1 South Cooler Calculation:

ASSAY SIMULATION FOR CELLS 1-5

C

[illegible]

C

C SIMULATION OF CELLS 1-5 WITH Pu-238 GAMMA SOURCES (99, 153, AND C 766 keV LINES ONLY). VARIED SOURCE DISTRIBUTIONS AND QUANTITIES OF C ATTENUATING MATERIALS WILL BE SIMULATED TO ESTIMATE UNCERTAINTY.

C

C GIRDERS BENEATH CELLS ARE SIMULATED AS A UNIFORM LAYER OF CARBON STEEL
C THE DENSITY OF THIS LAYER WAS ESTIMATED USING THE LENGTH OF GIRDER
C MATERIAL FOUND IN EACH CELL FROM DRAWINGS. THE GIRDER CHANNEL STOCK
C USED WAS NOMINALLY 4.1 LBS/FT.

C

C CELL GIRDER DENSITY (g/cm³)

C 1	0.321
-----	-------

C 2	0.393
-----	-------

C 3	0.315
-----	-------

C 4	0.286
-----	-------

C 5	0.150
-----	-------

C

C COOLED STORAGE UNITS IN CELLS 3-5 WILL BE SIMULATED BY REMOVING THE
C INTERIOR STORAGE COMPONENTS AND DOUBLING THE THICKNESS OF THE OUTER
C WALL (TO 1/2 INCH). THE COOLERS ARE FILLED WITH WATER. BASED ON ASSAY
C DATA, NOT HOLDUP IS LOCATED IN THESE CELLS

C

C COOLED STORAGE UNITS IN CELLS 1 AND 2 WILL BE MODELED EXPLICITLY.

C

C FURNACES WERE PRODUCED AS UNIVERSE 1.

C COLLIMATORS WERE PRODUCED AS UNIVERSE 2.

CPU-238 WELLS IN CELL 1 COOLER ARE UNIVERSE 3.

C CELL 1 COOLER IS UNIVERSE 4.

C PU-238 WELLS IN CELL 2 COOLER ARE UNIVERSE 5.

C CELL 2 COOLER IS UNIVERSE 6.

C TRANSLATION CARDS DEFINE CELL LOCATIONS.

C

C CELLS ARE FILLED WITH STAINLESS STEEL MATERIAL UP TO 30 cm IN ALL C CELLS. DENSITY OF THIS MATERIAL IS BASED ON WEIGHT ESTIMATES FROM C CELL INVENTORIES.

C

C MID RANGE ESTIMATES

C

C CELL MATERIAL FILL DENSITY (g/cm³)

C

C 1 0.083

C 2 0.044

C 3 0.020

C 4 0.026

C 5 0.083

C

C POINT SOURCES ARE LOCATED IN THE CELL 1 COOLER WELLS 3 CM

C

C CELL 5

C

50 800 -0.001205 47 -41 49 IMP:P=1 \$ INTERIOR
51 100 -7.92 -42 41 IMP:P=1 \$ WALLS
52 200 -0.150 -43 46 IMP:P=1 \$ GIRDERS
53 700 -1.0 -45 IMP:P=1 \$ COOLER INTERIOR
54 100 -7.92 -44 45 IMP:P=1 \$ COOLER WALLS
55 800 -0.001205 -46 #78 IMP:P=1 \$ FURNACE CUTOUT
56 100 -0.083 -41 -47 IMP:P=1 \$ MATERIAL FILL
57 400 -0.02 -48 IMP:P=1 \$ HEPA
58 100 -7.92 48 -49 IMP:P=1 \$ HEPA BOX

C

C FURNACES

C

60 100 -8.0 -51 52 U=1 IMP:P=1 \$ SKIN
61 700 -1.0 -52 65 U=1 IMP:P=1 \$ SHELL GAP (WATER FILLED)
62 100 -8.0 -53 54 U=1 IMP:P=1 \$ INNER SHELL
63 500 -0.76 -54 55 56 U=1 IMP:P=1 \$ ALUMINA BUBBLES
64 600 -8.06 -55 56 U=1 IMP:P=1 \$ HEATING ELEMENT
65 500 -3.85 -56 57 U=1 IMP:P=1 \$ HEATER TUBE
66 800 -0.001205 -57 58 U=1 IMP:P=1 \$ AIR GAP
67 500 -3.85 -58 59 U=1 IMP:P=1 \$ WORK TUBE
68 500 -0.84 -62 U=1 IMP:P=1 \$ SAMPLE HOLDER
69 800 -0.001205 62 -59 60 -63 U=1 IMP:P=1 \$ VOID SPACE 1
70 800 -0.001205 -61 U=1 IMP:P=1 \$ INSIDE SAMP. SUPP. TUBE
71 500 -3.85 -60 61 U=1 IMP:P=1 \$ SAMP. SUPP. TUBE
72 500 -3.85 60 -59 63 -64 U=1 IMP:P=1 \$ WORK TUBE INSULATION
73 800 -0.001205 60 -59 64 U=1 IMP:P=1 \$ VOID SPACE 2
74 100 -8.0 -65 66 U=1 IMP:P=1 \$ MIDDLE SHELL
75 800 -0.001205 -66 53 U=1 IMP:P=1 \$ SHELL GAP (AIR FILLED)
76 0 -67 FILL=1 TRCL=1 IMP:P=1 \$ FURNACE 1 CELL 1
77 0 -67 FILL=1 TRCL=2 IMP:P=1 \$ FURNACE 2 CELL 1
78 0 -67 FILL=1 TRCL=3 IMP:P=1 \$ FURNACE CELL 5
79 800 -0.001205 51 U=1 IMP:P=1 \$ OUTSIDE FURNACE

C

C COLLIMATOR

C

80 0 (-73:-70) 77 U=2 IMP:P=1 \$ COLLIMATOR VOID
81 100 -7.92 -71 70 U=2 IMP:P=1 \$ STEEL COLLIMATOR TUBE
82 900 -9.6 -72 71 73 U=2 IMP:P=1 \$ TUNGSTEN SHOT
83 0 -76 FILL=2 TRCL=4 IMP:P=1 \$ CELL 1 COLLIMATOR 2
84 0 -76 FILL=2 TRCL=5 IMP:P=1 \$ CELL 1 COLLIMATOR 3
85 0 -76 FILL=2 TRCL=6 IMP:P=1 \$ CELL 1 COLLIMATOR 4
86 0 -76 FILL=2 TRCL=7 IMP:P=1 \$ CELL 1 COLLIMATOR 5
87 0 -76 FILL=2 TRCL=8 IMP:P=1 \$ CELL 1 COLLIMATOR 6
88 0 -76 FILL=2 TRCL=9 IMP:P=1 \$ CELL 1 COLLIMATOR 8
89 0 -76 FILL=2 TRCL=10 IMP:P=1 \$ CELL 1 COLLIMATOR 9
90 0 -76 FILL=2 TRCL=11 IMP:P=1 \$ CELL 1 COLLIMATOR 10
91 0 -76 FILL=2 TRCL=12 IMP:P=1 \$ CELL 1 COLLIMATOR 11
92 0 -76 FILL=2 TRCL=13 IMP:P=1 \$ CELL 1 COLLIMATOR 12
93 0 -76 FILL=2 TRCL=14 IMP:P=1 \$ CELL 1 COLLIMATOR 13
94 0 -76 FILL=2 TRCL=15 IMP:P=1 \$ CELL 1 COLLIMATOR 14

95 0	-76 FILL=2	TRCL=16	IMP:P=1	\$ CELL 1 COLLIMATOR 15
96 0	-76 FILL=2	TRCL=17	IMP:P=1	\$ CELL 1 COLLIMATOR 16
97 0	-76 FILL=2	TRCL=18	IMP:P=1	\$ CELL 1 COLLIMATOR 17
98 0	-76 FILL=2	TRCL=19	IMP:P=1	\$ CELL 1 COLLIMATOR 18
99 0	-76 FILL=2	TRCL=20	IMP:P=1	\$ CELL 1 COLLIMATOR 19
100 0	-76 FILL=2	TRCL=21	IMP:P=1	\$ CELL 1 COLLIMATOR 20
101 0	-76 FILL=2	TRCL=22	IMP:P=1	\$ CELL 1 COLLIMATOR 21
102 0	-76 FILL=2	TRCL=23	IMP:P=1	\$ CELL 1 COLLIMATOR 22
103 0	-76 FILL=2	TRCL=24	IMP:P=1	\$ CELL 1 COLLIMATOR 23
104 0	-76 FILL=2	TRCL=25	IMP:P=1	\$ CELL 1 COLLIMATOR 24
105 0	-76 FILL=2	TRCL=26	IMP:P=1	\$ CELL 1 COLLIMATOR 25
106 0	-76 FILL=2	TRCL=27	IMP:P=1	\$ CELL 1 COLLIMATOR 26
107 0	-76 FILL=2	TRCL=28	IMP:P=1	\$ CELL 1 COLLIMATOR 27
108 0	-76 FILL=2	TRCL=29	IMP:P=1	\$ CELL 1 COLLIMATOR 28
109 0	-76 FILL=2	TRCL=30	IMP:P=1	\$ CELL 1 COLLIMATOR 29
110 0	-76 FILL=2	TRCL=31	IMP:P=1	\$ CELL 1 COLLIMATOR 30
111 0	-76 FILL=2	TRCL=32	IMP:P=1	\$ CELL 1 COLLIMATOR 31
112 0	-76 FILL=2	TRCL=33	IMP:P=1	\$ CELL 2 COLLIMATOR 32
113 0	-76 FILL=2	TRCL=34	IMP:P=1	\$ CELL 2 COLLIMATOR 33
114 0	-76 FILL=2	TRCL=35	IMP:P=1	\$ CELL 2 COLLIMATOR 34
115 0	-76 FILL=2	TRCL=36	IMP:P=1	\$ CELL 2 COLLIMATOR 35
116 0	-76 FILL=2	TRCL=37	IMP:P=1	\$ CELL 2 COLLIMATOR 36
117 0	-76 FILL=2	TRCL=38	IMP:P=1	\$ CELL 2 COLLIMATOR 37
118 0	-76 FILL=2	TRCL=39	IMP:P=1	\$ CELL 2 COLLIMATOR 38
119 0	-76 FILL=2	TRCL=40	IMP:P=1	\$ CELL 2 COLLIMATOR 39
120 0	-76 FILL=2	TRCL=41	IMP:P=1	\$ CELL 2 COLLIMATOR 40
121 0	-76 FILL=2	TRCL=42	IMP:P=1	\$ CELL 2 COLLIMATOR 41
122 0	-76 FILL=2	TRCL=43	IMP:P=1	\$ CELL 3 COLLIMATOR 1
123 0	-76 FILL=2	TRCL=44	IMP:P=1	\$ CELL 3 COLLIMATOR 2
124 0	-76 FILL=2	TRCL=45	IMP:P=1	\$ CELL 3 COLLIMATOR 3
125 0	-76 FILL=2	TRCL=46	IMP:P=1	\$ CELL 3 COLLIMATOR 4
126 0	-76 FILL=2	TRCL=47	IMP:P=1	\$ CELL 3 COLLIMATOR 5
127 0	-76 FILL=2	TRCL=48	IMP:P=1	\$ CELL 3 COLLIMATOR 6
128 0	-76 FILL=2	TRCL=49	IMP:P=1	\$ CELL 3 COLLIMATOR 7
129 0	-76 FILL=2	TRCL=50	IMP:P=1	\$ CELL 3 COLLIMATOR 8
130 0	-76 FILL=2	TRCL=51	IMP:P=1	\$ CELL 3 COLLIMATOR 9
131 0	-76 FILL=2	TRCL=52	IMP:P=1	\$ CELL 3 COLLIMATOR 10
132 0	-76 FILL=2	TRCL=53	IMP:P=1	\$ CELL 4 COLLIMATOR 11
133 0	-76 FILL=2	TRCL=54	IMP:P=1	\$ CELL 4 COLLIMATOR 12
134 0	-76 FILL=2	TRCL=55	IMP:P=1	\$ CELL 4 COLLIMATOR 13
135 0	-76 FILL=2	TRCL=56	IMP:P=1	\$ CELL 4 COLLIMATOR 14
136 0	-76 FILL=2	TRCL=57	IMP:P=1	\$ CELL 4 COLLIMATOR 15
137 0	-76 FILL=2	TRCL=58	IMP:P=1	\$ CELL 4 COLLIMATOR 16
138 0	-76 FILL=2	TRCL=59	IMP:P=1	\$ CELL 4 COLLIMATOR 17
139 0	-76 FILL=2	TRCL=60	IMP:P=1	\$ CELL 4 COLLIMATOR 18
140 0	-76 FILL=2	TRCL=61	IMP:P=1	\$ CELL 4 COLLIMATOR 19
141 0	-76 FILL=2	TRCL=62	IMP:P=1	\$ CELL 4 COLLIMATOR 20
142 0	-76 FILL=2	TRCL=63	IMP:P=1	\$ CELL 4 COLLIMATOR 21
143 0	-76 FILL=2	TRCL=64	IMP:P=1	\$ CELL 4 COLLIMATOR 22
144 0	-76 FILL=2	TRCL=65	IMP:P=1	\$ CELL 4 COLLIMATOR 23
145 0	-76 FILL=2	TRCL=66	IMP:P=1	\$ CELL 5 COLLIMATOR 24
146 0	-76 FILL=2	TRCL=67	IMP:P=1	\$ CELL 5 COLLIMATOR 25
147 0	-76 FILL=2	TRCL=68	IMP:P=1	\$ CELL 5 COLLIMATOR 26

148 0 -76 FILL=2 TRCL=69 IMP:P=1 \$ CELL 5 COLLIMATOR 27
 149 0 -76 FILL=2 TRCL=70 IMP:P=1 \$ CELL 5 COLLIMATOR 28
 150 0 -76 FILL=2 TRCL=71 IMP:P=1 \$ CELL 5 COLLIMATOR 29
 151 0 -76 FILL=2 TRCL=72 IMP:P=1 \$ CELL 5 COLLIMATOR 30
 152 0 -76 FILL=2 TRCL=73 IMP:P=1 \$ CELL 5 COLLIMATOR 31
 230 0 -76 FILL=2 TRCL=92 IMP:P=1 \$ CELL 1 COOLER COLLIMATOR
 231 0 -76 FILL=2 TRCL=93 IMP:P=1 \$ CELL 2.1 COOLER COLLIMATOR
 232 0 -76 FILL=2 TRCL=94 IMP:P=1 \$ CELL 2.2 COOLER COLLIMATOR
 233 0 -76 FILL=2 TRCL=95 IMP:P=1 \$ CELL 3 COOLER COLLIMATOR
 234 0 -76 FILL=2 TRCL=96 IMP:P=1 \$ CELL 4 COOLER COLLIMATOR
 235 0 -76 FILL=2 TRCL=97 IMP:P=1 \$ CELL 5 FURNACE COLLIMATOR
 153 800 -0.001205 72 U=2 IMP:P=1 \$ OUTSIDE COLLIMATOR
 154 0 -77 U=2 IMP:P=1 \$ DETECTION REGION
 C
 C CELL 1 COOLER
 C
 158 700 -1.0 85 83 U=3 IMP:P=1 \$ OUTSIDE WELL
 159 800 -0.001205 81 U=4 IMP:P=1 \$ OUTSIDE COOLER
 160 800 -0.001205 -82 U=3 IMP:P=1 \$ INNER PU-238 WELL
 161 100 -7.92 -83 82 U=3 IMP:P=1 \$ PU-238 WELL WALL
 162 100 -7.92 -85 83 U=3 IMP:P=1 \$ ENDCAP
 164 0 -84 U=4 FILL=3 TRCL=75 IMP:P=1 \$ WELL 1
 165 0 -84 U=4 FILL=3 TRCL=76 IMP:P=1 \$ WELL 2
 166 0 -84 U=4 FILL=3 TRCL=77 IMP:P=1 \$ WELL 3
 167 0 -84 U=4 FILL=3 TRCL=78 IMP:P=1 \$ WELL 4
 168 0 -84 U=4 FILL=3 TRCL=79 IMP:P=1 \$ WELL 5
 169 0 -84 U=4 FILL=3 TRCL=80 IMP:P=1 \$ WELL 6
 170 0 -84 U=4 FILL=3 TRCL=81 IMP:P=1 \$ WELL 7
 171 0 -84 U=4 FILL=3 TRCL=82 IMP:P=1 \$ WELL 8
 172 0 -84 U=4 FILL=3 TRCL=83 IMP:P=1 \$ WELL 9
 173 0 -84 U=4 FILL=3 TRCL=84 IMP:P=1 \$ WELL 10
 174 0 -84 U=4 FILL=3 TRCL=85 IMP:P=1 \$ WELL 11
 175 0 -84 U=4 FILL=3 TRCL=86 IMP:P=1 \$ WELL 12
 176 100 -7.92 -81 80 U=4 IMP:P=1 \$ COOLER WALL
 177 700 -1.0 #164 #165 #166 #167
 #168 #169 #170 #171
 #172 #173 #174 #175
 -80 U=4 IMP:P=1 \$ INSIDE COOLER
 178 0 -78 FILL=4 TRCL=74 IMP:P=1 \$ CELL 1 COOLER
 C
 C CELL 2 COOLER
 C
 180 800 -0.001205 -88 U=5 IMP:P=1 \$ INNER PU-238 WELL
 181 100 -7.92 -89 88 U=5 IMP:P=1 \$ PU-238 WELL WALL
 182 100 -7.92 -91 89 U=5 IMP:P=1 \$ ENDCAP
 184 0 -90 U=6 FILL=5 TRCL=88 IMP:P=1 \$ WELL 1
 185 0 -90 U=6 FILL=5 TRCL=89 IMP:P=1 \$ WELL 2
 186 0 -90 U=6 FILL=5 TRCL=90 IMP:P=1 \$ WELL 3
 187 0 -90 U=6 FILL=5 TRCL=91 IMP:P=1 \$ WELL 4
 188 100 -7.92 -87 86 U=6 IMP:P=1 \$ COOLER WALL
 189 700 -1.0 #184 #185 #186 #187
 -86 U=6 IMP:P=1 \$ INSIDE COOLER
 190 0 -79 FILL=6 TRCL=87 IMP:P=1 \$ CELL 2 COOLER

191 700 -1.0	91 89	U=5	IMP:P=1	\$ OUTSIDE WELL
192 800 -0.001205	87	U=6	IMP:P=1	\$ OUTSIDE COOLER
C				
C CELL 2 LARGE COOLER				
C				
200 800 -0.001205	-94		IMP:P=1	\$ INNER PU-238 WELL
201 100 -7.92	-95 94		IMP:P=1	\$ PU-238 WELL WALL
202 100 -7.92	-96 -97 95		IMP:P=1	\$ PU-238 WELL ENDCAP
203 700 -1.0	-96 97 95		IMP:P=1	\$ WATER SURROUNDING WELL
204 700 -1.0	-92 96		IMP:P=1	\$ INSIDE COOLER
205 100 -7.92	-93 92		IMP:P=1	\$ COOLER WALL
206 300 -11.34	-98 93		IMP:P=1	\$ LEAD JACKET
C				
C TRANSFER TUBES				
C				
210 800 -0.001205	-68 -6		IMP:P=1	\$ INNER TUBE CELLS 1-2
211 800 -0.001205	-68 -16		IMP:P=1	\$ INNER TUBE CELLS 2-3
212 800 -0.001205	-68 -26		IMP:P=1	\$ INNER TUBE CELLS 3-4
213 800 -0.001205	-68 -36		IMP:P=1	\$ INNER TUBE CELLS 4-5
214 100 -7.92	-69 68 -6		IMP:P=1	\$ INNER TUBE CELLS 1-2
215 100 -7.92	-69 68 -16		IMP:P=1	\$ INNER TUBE CELLS 2-3
216 100 -7.92	-69 68 -26		IMP:P=1	\$ INNER TUBE CELLS 3-4
217 100 -7.92	-69 68 -36		IMP:P=1	\$ INNER TUBE CELLS 4-5
C				
C VOID CELLS				
C				
996 800 -0.001205	-101 -75		IMP:P=1	\$ VOID BENEATH COLLIMATORS
997 800 -0.001205	#83 #84 #85 #86 #87			
	#88 #89 #90 #91 #92			
	#93 #94 #95 #96 #97			
	#98 #99 #100 #101 #102			
	#103 #104 #105 #106 #107			
	#108 #109 #110 #111 #112			
	#113 #114 #115 #116 #117			
	#118 #119 #120 #121 #122			
	#123 #124 #125 #126 #127			
	#128 #129 #130 #131 #132			
	#133 #134 #135 #136 #137			
	#138 #139 #140 #141 #142			
	#143 #144 #145 #146 #147			
	#148 #149 #150 #151 #152			
	-101 -74 75		IMP:P=1	\$ VOID SURROUNDING COLLIMATORS
998 800 -0.001205	-101 100 24 34 44			
	#76 #77 #78 74 #178			
	#190 98 #230 #231 #232			
	#233 #234 #235		IMP:P=1	\$ VOID SURROUNDING CELLS
999 0	101		IMP:P=0	\$ THE GRAVEYARD

[illegible]

C

C CELL 1

C

1 RPP 0. 512.45 0. 152.4 0. 208.28 \$ INTERIOR
2 RPP -0.32 512.76 -0.32 152.72 -0.476 208.6 \$ EXTERIOR
3 RPP -0.32 512.76 -0.32 152.72 -8.096 -0.476 \$ GIRDERS
4 RPP 36.83 90.17 90.17 143.51 -8.096 -0.476 \$ FURNACE 1 CUTOUT
5 RPP 322.26 375.60 90.17 143.51 -8.096 -0.476 \$ FURNACE 2 CUTOUT
6 RPP 512.76 523.88 -0.32 152.72 -8.096 208.6 \$ CELL GAP
7 PZ 30 \$ MATERIAL FILL
8 RPP 266.84 297.03 131.45 147.00 89.52 119.71 \$ INNER HEPA
9 RPP 266.54 297.34 131.45 147.00 89.22 120.02 \$ HEPA BOX

C

C CELL 2

C

11 RPP 524.19 726.12 0. 152.4 0. 208.28 \$ INTERIOR
12 RPP 523.88 726.44 -0.32 152.72 -0.476 208.6 \$ EXTERIOR
13 RPP 523.88 726.44 -0.32 152.72 -8.096 -0.476 \$ GIRDERS
16 RPP 726.44 737.55 -0.32 152.72 -8.096 208.6 \$ CELL GAP
17 PZ 30 \$ MATERIAL FILL
18 RPP 641.81 672.00 131.45 147.00 89.52 119.71 \$ INNER HEPA
19 RPP 641.51 672.31 131.45 147.00 89.22 120.02 \$ HEPA BOX

C

C CELL 3

C

21 RPP 737.87 939.80 0. 152.4 0. 208.28 \$ INTERIOR
22 RPP 737.55 940.12 -0.32 152.72 -0.476 208.6 \$ EXTERIOR
23 RPP 737.55 940.12 -0.32 152.72 -8.096 -0.476 \$ GIRDERS
24 RCC 785.50 52.07 -8.096 0. 0. -50.96 24.13 \$ COOLER EXT
25 RCC 785.50 52.07 -8.096 0. 0. -49.45 22.62 \$ COOLER INT
26 RPP 940.12 951.23 -0.32 152.72 -8.096 208.6 \$ CELL GAP
27 PZ 30 \$ MATERIAL FILL
28 RPP 790.72 820.91 131.45 147.00 89.52 119.71 \$ INNER HEPA
29 RPP 790.42 821.21 131.45 147.00 89.22 120.02 \$ HEPA BOX

C

C CELL 4

C

31 RPP 951.55 1215.39 0. 152.4 0. 208.28 \$ INTERIOR
32 RPP 951.23 1215.71 -0.32 152.72 -0.476 208.6 \$ EXTERIOR
33 RPP 951.23 1215.71 -0.32 152.72 -8.096 -0.476 \$ GIRDERS
34 RCC 1170.15 52.07 -8.096 0. 0. -50.96 27.94 \$ COOLER EXT
35 RCC 1170.15 52.07 -8.096 0. 0. -49.45 26.43 \$ COOLER INT
36 RPP 1215.71 1226.82 -0.32 152.72 -8.096 208.6 \$ CELL GAP
37 PZ 30 \$ MATERIAL FILL
38 RPP 1073.45 1103.64 131.45 147.00 89.52 119.71 \$ INNER HEPA
39 RPP 1073.15 1103.95 131.45 147.00 89.22 120.02 \$ HEPA BOX

C

C CELL 5

C

41 RPP 1227.14 1501.46 0. 152.4 0. 208.28 \$ INTERIOR
42 RPP 1226.82 1501.78 -0.32 152.72 -0.476 208.6 \$ EXTERIOR
43 RPP 1226.82 1501.78 -0.32 152.72 -8.096 -0.476 \$ GIRDERS
44 RCC 1402.40 52.07 -8.096 0. 0. -50.96 27.94 \$ COOLER EXT

45 RCC 1402.40 52.07 -8.096 0. 0. -49.45 26.43 \$ COOLER INT
46 RPP 1264.29 1317.63 90.17 143.51 -8.096 -0.476 \$ FURNACE CUTOUT
47 PZ 30 \$ MATERIAL FILL
48 RPP 1308.56 1338.75 131.45 147.00 89.52 119.71 \$ INNER HEPA
49 RPP 1308.26 1339.06 131.45 147.00 89.22 120.02 \$ HEPA BOX
C
C FURNACE
C
51 RCC 0 0 -79.02 0 0 79.02 17.28 \$ SKIN OUTER SURFACE
52 RCC 0 0 -78.38 0 0 78.38 17.16 \$ SKIN INNER SURFACE
53 RCC 0 0 -78.07 0 0 78.07 15.88 \$ INNER SHELL OUTER SURFACE
54 RCC 0 0 -77.27 0 0 77.27 15.57 \$ INNER SHELL INNER SURFACE
55 RCC 0 0 -64.57 0 0 44.70 7.77 \$ HEATING ELEMENT OUTER
56 RCC 0 0 -67.11 0 0 67.11 7.62 \$ HEATER TUBE OUTER
57 RCC 0 0 -65.84 0 0 65.84 6.99 \$ HEATER TUBE INNER
58 RCC 0 0 -64.57 0 0 64.57 6.67 \$ WORK TUBE OUTER
59 RCC 0 0 -63.94 0 0 63.94 6.03 \$ WORK TUBE INNER
60 RCC 0 0 -35.11 0 0 35.11 1.91 \$ SAMPLE SUPPORT TUBE OUTER
61 RCC 0 0 -35.11 0 0 35.11 1.60 \$ SAMPLE SUPPORT TUBE INNER
62 RCC 0 0 -63.94 0 0 28.83 5.72 \$ SAMPLE HOLDER
63 PZ -31.30 \$ WORK TUBE LOWER INSUL.
64 PZ -24.95 \$ WORK TUBE UPPER INSUL.
65 RCC 0 0 -78.38 0 0 78.38 16.85 \$ MIDDLE SHELL OUTER SURFACE
66 RCC 0 0 -78.38 0 0 78.38 16.29 \$ MIDDLE SHELL INNER SURFACE
67 RCC 0 0 -79.021 0 0 79.022 17.281 \$ FURNACE FILL SURFACE
C
C TRANSFER TUBE
C
68 C/X 116.84 27.94 19.84 \$ INNER TRANSFER TUBE
69 C/X 116.84 27.94 20.32 \$ OUTER TRANSFER TUBE
C
C COLLIMATOR
C
70 RCC 0 0 0 0 -10.16 2.06 \$ INNER WALL CENTRAL TUBE
71 RCC 0 0 0 0 -10.16 2.22 \$ OUTER WALL CENTRAL TUBE
72 RCC 0 0 0 0 -15.88 8.41 \$ OUTER COLLIMATOR SURFACE
73 RCC 0 0 -10.16 0 0 -5.72 3.81 \$ DETECTOR VOID
74 PZ -94 \$ UPPER COLLIMATOR REGION
75 PZ -115 \$ LOWER COLLIMATOR REGION
76 RCC 0 0 0.001 0 0 -15.882 8.411 \$ COLLIMATOR FILL SURFACE
77 RCC 0 0 -10.16 0 0 -0.01 2.06 \$ DETECTION REGION
C
C CELL 1 COOLER
C
78 RCC 0 0 0.001 0 0 -59.212 30.481 \$ CELL 1 COOLER FILL SURFACE
79 RCC 0 0 0.001 0 0 -50.962 23.501 \$ CELL 2 COOLER FILL SURFACE
80 RCC 0 0 -1.43 0 0 -57.15 29.84 \$ INNER COOLER
81 RCC 0 0 0 0 -59.21 30.48 \$ OUTER COOLER
82 RCC 0 0 0 0 -46.36 2.24 \$ INNER WELL
83 RCC 0 0 0 0 -48.90 3.11 \$ OUTER WELL
84 RCC 0 0 0.001 0 0 -48.902 3.651 \$ WELL BOUNDING SURFACE
85 RCC 0 0 -45.09 0 0 -3.81 3.65 \$ ENDCAP
C

[illegible]

TR1	63.5	116.84	-0.482	\$ FURNACE 1 CELL 1
TR2	348.93	116.84	-0.482	\$ FURNACE 2 CELL 1
TR3	1290.96	116.84	-0.482	\$ FURNACE CELL 5
TR4	23.77	49.53	-94.46	\$ CELL 1 COLLIMATOR 2
TR5	19.91	74.30	-94.46	\$ CELL 1 COLLIMATOR 3
TR6	19.91	106.68	-94.46	\$ CELL 1 COLLIMATOR 4
TR7	77.79	40.96	-94.46	\$ CELL 1 COLLIMATOR 5
TR8	72.28	66.68	-94.46	\$ CELL 1 COLLIMATOR 6
TR9	105.35	40.96	-94.46	\$ CELL 1 COLLIMATOR 8
TR10	105.35	77.79	-94.46	\$ CELL 1 COLLIMATOR 9
TR11	105.35	111.44	-94.46	\$ CELL 1 COLLIMATOR 10
TR12	149.45	111.44	-94.46	\$ CELL 1 COLLIMATOR 11
TR13	164.15	77.79	-94.46	\$ CELL 1 COLLIMATOR 12
TR14	183.75	44.45	-94.46	\$ CELL 1 COLLIMATOR 13
TR15	193.55	77.79	-94.46	\$ CELL 1 COLLIMATOR 14
TR16	193.55	111.44	-94.46	\$ CELL 1 COLLIMATOR 15
TR17	235.20	111.44	-94.46	\$ CELL 1 COLLIMATOR 16
TR18	237.65	77.79	-94.46	\$ CELL 1 COLLIMATOR 17
TR19	235.20	43.82	-94.46	\$ CELL 1 COLLIMATOR 18
TR20	298.29	43.82	-94.46	\$ CELL 1 COLLIMATOR 19
TR21	298.29	77.79	-94.46	\$ CELL 1 COLLIMATOR 20
TR22	298.29	111.44	-94.46	\$ CELL 1 COLLIMATOR 21
TR23	333.81	77.79	-94.46	\$ CELL 1 COLLIMATOR 22
TR24	333.81	40.96	-94.46	\$ CELL 1 COLLIMATOR 23
TR25	369.95	40.96	-94.46	\$ CELL 1 COLLIMATOR 24
TR26	369.95	77.79	-94.46	\$ CELL 1 COLLIMATOR 25
TR27	367.01	111.44	-94.46	\$ CELL 1 COLLIMATOR 26
TR28	426.30	111.44	-94.46	\$ CELL 1 COLLIMATOR 27
TR29	432.12	77.79	-94.46	\$ CELL 1 COLLIMATOR 28
TR30	457.54	111.44	-94.46	\$ CELL 1 COLLIMATOR 29
TR31	474.69	88.27	-94.46	\$ CELL 1 COLLIMATOR 30
TR32	479.59	40.96	-94.46	\$ CELL 1 COLLIMATOR 31
TR33	518.32	116.52	-94.46	\$ CELL 2 COLLIMATOR 32
TR34	558.48	111.44	-94.46	\$ CELL 2 COLLIMATOR 33
TR35	558.48	75.25	-94.46	\$ CELL 2 COLLIMATOR 34
TR36	595.95	40.96	-94.46	\$ CELL 2 COLLIMATOR 35
TR37	625.79	118.11	-94.46	\$ CELL 2 COLLIMATOR 36
TR38	657.54	116.52	-94.46	\$ CELL 2 COLLIMATOR 37
TR39	668.34	81.28	-94.46	\$ CELL 2 COLLIMATOR 38
TR40	695.65	43.82	-94.46	\$ CELL 2 COLLIMATOR 39
TR41	695.65	76.20	-94.46	\$ CELL 2 COLLIMATOR 40
TR42	710.88	111.44	-94.46	\$ CELL 2 COLLIMATOR 41
TR43	759.14	78.74	-94.46	\$ CELL 3 COLLIMATOR 1
TR44	742.95	40.96	-94.46	\$ CELL 3 COLLIMATOR 2
TR45	795.66	80.01	-94.46	\$ CELL 3 COLLIMATOR 3
TR46	795.66	111.44	-94.46	\$ CELL 3 COLLIMATOR 4
TR47	854.08	111.44	-94.46	\$ CELL 3 COLLIMATOR 5
TR48	854.08	77.15	-94.46	\$ CELL 3 COLLIMATOR 6
TR49	852.49	40.96	-94.46	\$ CELL 3 COLLIMATOR 7
TR50	905.51	40.96	-94.46	\$ CELL 3 COLLIMATOR 8
TR51	905.51	76.20	-94.46	\$ CELL 3 COLLIMATOR 9
TR52	905.51	111.44	-94.46	\$ CELL 3 COLLIMATOR 10
TR53	974.41	111.44	-94.46	\$ CELL 4 COLLIMATOR 11

TR54	971.55	76.20	-94.46	\$ CELL 4 COLLIMATOR 12
TR55	977.27	40.96	-94.46	\$ CELL 4 COLLIMATOR 13
TR56	1034.42	40.96	-94.46	\$ CELL 4 COLLIMATOR 14
TR57	1034.42	80.01	-94.46	\$ CELL 4 COLLIMATOR 15
TR58	1034.42	111.44	-94.46	\$ CELL 4 COLLIMATOR 16
TR59	1083.95	111.44	-94.46	\$ CELL 4 COLLIMATOR 17
TR60	1083.95	76.20	-94.46	\$ CELL 4 COLLIMATOR 18
TR61	1084.26	40.96	-94.46	\$ CELL 4 COLLIMATOR 19
TR62	1131.25	40.96	-94.46	\$ CELL 4 COLLIMATOR 20
TR63	1141.10	88.58	-94.46	\$ CELL 4 COLLIMATOR 21
TR64	1158.24	111.44	-94.46	\$ CELL 4 COLLIMATOR 22
TR65	1210.31	116.84	-94.46	\$ CELL 4 COLLIMATOR 23
TR66	1241.43	40.96	-94.46	\$ CELL 5 COLLIMATOR 24
TR67	1229.68	72.39	-94.46	\$ CELL 5 COLLIMATOR 25
TR68	1260.79	111.44	-94.46	\$ CELL 5 COLLIMATOR 26
TR69	1261.43	71.44	-94.46	\$ CELL 5 COLLIMATOR 27
TR70	1304.29	76.20	-94.46	\$ CELL 5 COLLIMATOR 28
TR71	1330.01	40.96	-94.46	\$ CELL 5 COLLIMATOR 29
TR72	1389.70	105.73	-94.46	\$ CELL 5 COLLIMATOR 30
TR73	1402.40	77.72	-94.46	\$ CELL 5 COLLIMATOR 31
TR74	447.99	52.07	-0.482	\$ CELL 1 COOLER
TR75	0.0	8.53	-1.432	\$ WELL 1 CELL 1 COOLER
TR76	8.53	0.0	-1.432	\$ WELL 2 CELL 1 COOLER
TR77	-8.53	0.0	-1.432	\$ WELL 3 CELL 1 COOLER
TR78	0.0	-8.53	-1.432	\$ WELL 4 CELL 1 COOLER
TR79	-8.53	17.06	-1.432	\$ WELL 5 CELL 1 COOLER
TR80	8.53	17.06	-1.432	\$ WELL 6 CELL 1 COOLER
TR81	17.06	-8.53	-1.432	\$ WELL 7 CELL 1 COOLER
TR82	17.06	8.53	-1.432	\$ WELL 8 CELL 1 COOLER
TR83	8.53	-17.06	-1.432	\$ WELL 9 CELL 1 COOLER
TR84	-8.53	-17.06	-1.432	\$ WELL 10 CELL 1 COOLER
TR85	-17.06	8.53	-1.432	\$ WELL 11 CELL 1 COOLER
TR86	-17.06	-8.53	-1.432	\$ WELL 12 CELL 1 COOLER
TR87	561.66	52.07	-0.482	\$ CELL 2 COOLER
TR88	7.62	7.62	-1.432	\$ WELL 1 CELL 2 COOLER
TR89	7.62	-7.62	-1.432	\$ WELL 2 CELL 2 COOLER
TR90	-7.62	7.62	-1.432	\$ WELL 3 CELL 2 COOLER
TR91	-7.62	-7.62	-1.432	\$ WELL 4 CELL 2 COOLER
TR92	447.99	-17.78	-55.09	
	1	0	0	
	0	0	-1	
	0	1	0	\$ CELL 1 COOLER COLLIMATOR
TR93	561.66	3.18	-41.12	
	1	0	0	
	0	0	-1	
	0	1	0	\$ CELL 2.1 COOLER COLLIMATOR
TR94	634.05	-37.15	-42.07	
	1	0	0	
	0	0	-1	
	0	1	0	\$ CELL 2.2 COOLER COLLIMATOR
TR95	785.50	-33.02	-41.75	
	1	0	0	
	0	0	-1	

	0	1	0	\$ CELL 3 COOLER COLLIMATOR
TR96	1170.15	-36.02	-41.75	
	1	0	0	
	0	0	-1	
	0	1	0	\$ CELL 4 COOLER COLLIMATOR
TR97	1290.96	266.30	-41.75	
	1	0	0	
	0	0	1	
	0	-1	0	\$ CELL 5 FURNACE COLLIMATOR
C				
C	CC			
C				
C	MATERIAL CARDS			
C				
C	CC			
C				
C	STAINLESS STEEL 316, DENSITY = 7.92 g/cm^3			
C				
M100	14000	-0.010	\$ Si	
	24000	-0.170	\$ Cr	
	25000	-0.020	\$ Mn	
	26000	-0.655	\$ Fe	
	28000	-0.120	\$ Ni	
	42000	-0.025	\$ Mo	
C				
C	CARBON STEEL, DENSITY = 7.82 g/cc			
C				
M200	6000	-0.005	\$ C	
	26000	-0.995	\$ Fe	
C				
C	LEAD, DENSITY = 11.34 g/cm^3			
C				
M300	82000	1.0	\$ Pb	
C				
C	BOROSILICATE FIBERGLASS FILTER, DENSITY = 0.02 g/cm^3			
C				
M400	5000	-0.040063	\$ B	
	8000	-0.539561	\$ O	
	11000	-0.028191	\$ Na	
	13000	-0.011644	\$ Al	
	14000	-0.377220	\$ Si	
	19000	-0.003321	\$ K	
C				
C				
C	ALUMINUM OXIDE, DENSITY = 3.75-3.95 g/cm^3			
C				
M500	8000	0.6	\$ O	
	13000	0.4	\$ Al	
C				
C	TUNGSTEN, DENSITY = 19.3 g/cm^3			
C				
M600	74000	1.0	\$ W	
C				

```
C WATER, DENISTY = 1.0 g/cm^3
C
M700    1000   0.666667   $ H
        8000   0.333333   $ O
C
C AIR, DENSITY = 0.001205 g/cm^3
C
M800     6000   0.000124   $ C
        7000   0.755268   $ N
            8000   0.231781   $ O
            18000  0.012827   $ Ar
C
C TUNGSTEN SHOT : BULK DENSITY = 9.6 g/cc
C
M900 26000 -0.1    $ Fe
      28000 -0.2    $ Ni
      74000 -0.7    $ W
C
C CCCCCCCCCCCCCCCCCCCCCCCCCCCCCCCCCCCCCCCCCCCCCCCCCCCCCCCCCCCCCCC
C
C SOURCE CARDS
C
C CCCCCCCCCCCCCCCCCCCCCCCCCCCCCCCCCCCCCCCCCCCCCCCCCCCCCCCCCCCCCCC
C
C
SDEF PAR=P          $ PHOTON SOURCE
    ERG=D1         $ ENERGY GIVEN BY DISTRIBUTION 1
    POS=D2         $ POINT SOURCES
C
C ENERGY DISTRIBUTION (DISCRETE LINES)
C
SI1 L 0.099853
      0.152720
      0.76639
C
C ENERGY DISTRIBUTION PROBABILITIES (UNNORMALIZED)
C
SP1  1.
     1.
     1.
C
C POINT SOURCE LOCATIONS
C
SI2 L 447.99 60.60 -45.26
      456.52 52.07 -45.26
      439.46 52.07 -45.26
      447.99 43.54 -45.26
      439.46 69.13 -45.26
      456.52 69.13 -45.26
      465.05 43.54 -45.26
      465.05 60.60 -45.26
      456.52 35.01 -45.26
      439.46 35.01 -45.26
```

430.93	00.00	-45.20
430.93	43.54	-45.26

C SOURCE LOCATION PROBABILITIES (UNNORMALIZED)

SP2 1.

1.

1.

1.

1.

1.

[illegible]

C TALLY CARDS

C CCC

E5 0. 0.099 0.1 0.152 0.153 0.766 0.767 \$ TALLY 5 ENERGY BINS

FC5 PHOTON FLUX AT CELL 1 ASSAY POSITIONS

F5:P 23.77 49.53 -104.62 0

19.91 106.68 -104.62 0

72.28 66.68 -104.62 0

105.35 77.79 -104.62 0

149.45 111.44 -104.62 0

183.75 44.45 -104.62 0

193.55 111.44 -104.62 0

237.65 77.79 -104.62 0

298.29 43.82 -104.62 0
298.29 43.82 -104.62 0298.29 111.44 -104.02 0
233.81 57.70 -104.62 0

355.01	40.90	104.62 0
360.05	40.06	104.62 0

367.01 111.44 -104.62.0

426 30 111 44 -104 62 0

432.12 77.79 -104.62 0
457.54 111.44 -104.62 0
474.69 88.27 -104.62 0
479.59 40.96 -104.62 0

C

E15 0. 0.099 0.1 0.152 0.153 0.766 0.767 \$ TALLY 15 ENERGY BINS

C

FC15 PHOTON FLUX AT CELL 2 ASSAY POSITIONS

C

F15:P 518.32 116.52 -104.62 0

558.48 111.44 -104.62 0
558.48 75.25 -104.62 0
595.95 40.96 -104.62 0
625.79 118.11 -104.62 0
657.54 116.52 -104.62 0
668.34 81.28 -104.62 0
695.65 43.82 -104.62 0
695.65 76.20 -104.62 0
710.88 111.44 -104.62 0

C

E25 0. 0.099 0.1 0.152 0.153 0.766 0.767 \$ TALLY 25 ENERGY BINS

C

FC25 PHOTON FLUX AT CELL 3 ASSAY POSITIONS

C

F25:P 759.14 78.74 -104.62 0

742.95 40.96 -104.62 0
795.66 80.01 -104.62 0
795.66 111.44 -104.62 0
854.08 111.44 -104.62 0
854.08 77.15 -104.62 0
852.49 40.96 -104.62 0
905.51 40.96 -104.62 0
905.51 76.20 -104.62 0
905.51 111.44 -104.62 0

C

E35 0. 0.099 0.1 0.152 0.153 0.766 0.767 \$ TALLY 35 ENERGY BINS

C

FC35 PHOTON FLUX AT CELL 4 ASSAY POSITIONS

C

F35:P 974.41 111.44 -104.62 0

971.55 76.20 -104.62 0
977.27 40.96 -104.62 0
1034.42 40.96 -104.62 0
1034.42 80.01 -104.62 0
1034.42 111.44 -104.62 0
1083.95 111.44 -104.62 0
1083.95 76.20 -104.62 0
1084.26 40.96 -104.62 0
1131.25 40.96 -104.62 0
1141.10 88.58 -104.62 0
1158.24 111.44 -104.62 0
1210.31 116.84 -104.62 0

C

E45 0. 0.099 0.1 0.152 0.153 0.766 0.767 \$ TALLY 45 ENERGY BINS

C

FC45 PHOTON FLUX AT CELL 5 ASSAY POSITIONS

C

F45:P 1241.43 40.96 -104.62 0

1229.68 72.39 -104.62 0

1260.79 111.44 -104.62 0

1261.43 71.44 -104.62 0

1304.29 76.20 -104.62 0

1330.01 40.96 -104.62 0

1389.70 105.73 -104.62 0

1402.40 77.72 -104.62 0

C

C

E55 0. 0.099 0.1 0.152 0.153 0.766 0.767 \$ TALLY 45 ENERGY BINS

C

FC55 PHOTON FLUX AT COOLER ASSAY POSITIONS

C

F55:P 447.99 -27.94 -55.09 0

561.66 -6.99 -41.12 0

634.05 -47.31 -42.07 0

785.50 -43.18 -41.75 0

1170.15 -46.18 -41.75 0

1290.96 276.46 -41.75 0

C

FC4 PHOTON FLUX AT CELL 1 ASSAY POSITIONS (THIN DISK DETECTOR)

C

F4:P (154<83)

(154<84)

(154<85)

(154<86)

(154<87)

(154<88)

(154<89)

(154<90)

(154<91)

(154<92)

(154<93)

(154<94)

(154<95)

(154<96)

(154<97)

(154<98)

(154<99)

(154<100)

(154<101)

(154<102)

(154<103)

(154<104)

(154<105)

(154<106)

(154<107)

(154<108)

(154<109)
(154<110)
(154<111)
C
E4 0. 1998i 1.0 \$ DISK DETECTOR TALLY ENERGY BINS
C
C SPLITS TALLY 4 INTO THREE TALLIES ONE FOR EACH SOURCE ENERGY
C
FT4 SCX 1
C
FC14 PHOTON FLUX AT CELL 2 ASSAY POSITIONS (THIN DISK DETECTOR)
C
F14:P (154<112)
 (154<113)
 (154<114)
 (154<115)
 (154<116)
 (154<117)
 (154<118)
 (154<119)
 (154<120)
 (154<121)
C
E14 0. 1998i 1.0 \$ DISK DETECTOR TALLY ENERGY BINS
C
C SPLITS TALLY 14 INTO THREE TALLIES ONE FOR EACH SOURCE ENERGY
C
FT14 SCX 1
C
FC24 PHOTON FLUX AT CELL 3 ASSAY POSITIONS (THIN DISK DETECTOR)
C
F24:P (154<122)
 (154<123)
 (154<124)
 (154<125)
 (154<126)
 (154<127)
 (154<128)
 (154<129)
 (154<130)
 (154<131)
C
E24 0. 1998i 1.0 \$ DISK DETECTOR TALLY ENERGY BINS
C
C SPLITS TALLY 24 INTO THREE TALLIES ONE FOR EACH SOURCE ENERGY
C
FT24 SCX 1
C
FC34 PHOTON FLUX AT CELL 4 ASSAY POSITIONS (THIN DISK DETECTOR)
C
F34:P (154<132)
 (154<133)
 (154<134)

(154<135)
(154<136)
(154<137)
(154<138)
(154<139)
(154<140)
(154<141)
(154<142)
(154<143)
(154<144)

C

E34 0. 1998i 1.0 \$ DISK DETECTOR TALLY ENERGY BINS

C

C SPLITS TALLY 34 INTO THREE TALLIES ONE FOR EACH SOURCE ENERGY

C

FT34 SCX 1

C

FC44 PHOTON FLUX AT CELL 4 ASSAY POSITIONS (THIN DISK DETECTOR)

C

F44:P (154<145)

(154<146)
(154<147)
(154<148)
(154<149)
(154<150)
(154<151)
(154<152)

C

E44 0. 1998i 1.0 \$ DISK DETECTOR TALLY ENERGY BINS

C

C SPLITS TALLY 44 INTO THREE TALLIES ONE FOR EACH SOURCE ENERGY

C

FT44 SCX 1

C

FC54 PHOTON FLUX AT COOLER ASSAY POSITIONS (THIN DISK DETECTOR)

C

F54:P (154<230)

(154<231)
(154<232)
(154<233)
(154<234)
(154<235)

C

E54 0. 1998i 1.0 \$ DISK DETECTOR TALLY ENERGY BINS

C

C SPLITS TALLY 54 INTO THREE TALLIES ONE FOR EACH SOURCE ENERGY

C

FT54 SCX 1

Distribution:

A.H. Couture (PSC)

D.P. Diprete (773-41A)

R.S. Lee (773-41A)

J.C. Musall (707-7F)

E.T. Sadowski (773-A)

R.H. Young (773-A)

M.L. Gilles (707-7F)

Records Administration (EDWS)